15. GEOTECHNICAL PROPERTIES OF MIDDLE AMERICA TRENCH SEDIMENTS, DEEP SEA DRILLING PROJECT LEG 66[1]

L. E. Shephard,[2] W. R. Bryant, and W. A. Chiou, Department of Oceanography,
Texas A&M University, College Station, Texas

INTRODUCTION

Delineating the interrelationships between tectonics, sedimentation, and geotechnical properties is particularly important for areas subjected to the dynamic affects of convergence. DSDP Leg 66 drilling within the Middle America Trench complex provided a unique opportunity to investigate these interrelationships along a transect of eight drill sites beginning on the trench outer slope and traversing the trench, trench inner slope, and upper continental slope (Fig. 1). Investigations of other convergent margins suggest that deformation occurs most rapidly along the lower trench inner slope and is reflected by the geotechnical properties (Carson, 1977; Seely, 1977; and von Huene, 1979). This study focuses on the geotechnical properties of Middle America Trench sediments and the possible affects of convergence on these properties.

TECHNIQUES

Routine geotechnical property measurements, tabulated in the Appendix at the end of this chapter, include (1) bulk density (Mg/m^3), (2) porosity (%), (3) water content (% total weight), (4) undrained shear strength (kPa), and (5) compressional sound velocity (km/s). Shipboard measurements and computations were performed utilizing procedures, equipment, correction factors, and standards outlined by Boyce (1975, 1977). Evaluations, recurring problems, and sources of errors for many of these techniques are summarized by Bennett and Keller (1973) and Demars and Nacci (1977), hence only modifications to these procedures and specific problems pervasive to Leg 66 analyses will be discussed.

Good core recovery at most sites allowed regular sampling from least disturbed core sections. Core disturbance resulting from normal drilling and handling operations appeared limited, but some cored intervals of gassy sediments were very disturbed and displayed expansion features and erratic values of geotechnical properties. Technical problems prevented logging, except through the drill pipe, thus precluding any correlations with *in situ* physical properties. All index properties reported are uncorrected for salt content.

Bulk density and porosity were determined shipboard by continuous gamma ray attenuation of unsplit cores and by two-minute gamma ray and gravimetric analyses of rock chunk samples. Shore-based measurements were performed utilizing an air comparison pycnometer. *Initial Reports* volumes are replete with discussions of GRAPE (gamma ray attenuation and porosity evaluator) data. Although these data are presented graphically in the site chapters and in the geotechnical property summary tables at the conclusion of this chapter to follow previous DSDP format, all interpretations of porosity and bulk density data are based on gravimetric and air comparison pycnometer data. Grain and fluid densities of 2.70 Mg/m^3 and 1.025 Mg/m^3 were used in all shipboard GRAPE computations (Boyce, 1975).

Gravimetric and air comparison pycnometer samples were carefully selected to alleviate many of the problems associated with drilling disturbance. Gas-related sediment disturbance was often restricted in 2- to 3-meter zones, permitting sampling in least disturbed core subsections. Large samples (≥ 10 cm^3) improved reproducibility and confidence in volume measurements for porosity and bulk density computations. Sediment spalling and fissility with increased induration prevented some gravimetric measurements. Water content (% total weight) was determined for all samples analyzed gravimetrically or by the air comparison pycnometer. Large ($\simeq 20$ cm) rock chunk samples were also used for determining water content and porosity. Porosity values obtained from the rock chunk samples were computed assuming 100% sample saturation and using an average grain density value determined for major lithologic units at each site.

Undrained shear strengths were determined using a Wykeham-Farrance vane shear rotating 89° per minute and a Cl-600 Torvane. All measurements were performed parallel to bedding on split core sections. Premature sediment failure by cracking often prevented testing of samples having strengths greater than 100 kPa. Reasonably good agreement was obtained between vane shear and Torvane results.

Compressional sound velocity measurements, performed utilizing a Hamilton-Frame velocimeter emitting a 400-kHz sonic signal, were limited by signal attenuation due to gas, even over short (< 1 cm) travel paths. Most measured velocities are lower than those calculated from multichannel seismic reflection data, further decreasing confidence in shipboard measurements.

Consolidation tests were performed utilizing Anteus back-pressure consolidometers. The primary advantages of the Anteus unit and the general procedures employed can be found in Lowe et al. (1964) and Bowles (1970). Casagrande's technique (1936) was used to determine the preconsolidation pressure, P_c, which is the maximum pressure a sediment has been consolidated to in the past. Comparing the preconsolidation pressure to the effective overburden pressure P_o' (calculated assuming linear hydrostatic pore pressure conditions) determines the state of consolidation. According to soil mechanics terminology, a normally consolidated sediment has fully consolidated under the present effective overburden pressure ($P_c = P_o'$). Overconsolidated sediments have been consolidated to a pressure in excess of the present effective overburden pressure ($P_c > P_o'$). Underconsolidated sediments have not fully consolidated under the present effective overburden pressure ($P_c < P_o'$).

All consolidation test samples were carefully selected on the basis of minimum disturbance. Split cores above and below the consolidation sample (whole round core segment) were examined visually shipboard to determine qualitatively the relative degree of sediment disturbance. Prior to testing in the laboratory all core samples were radiographed to further delineate core quality and potential core disturbance. Despite these precautions core disturbance does occur, especially in zones of high gas content.

Index of disturbance I_D, a technique for quantifying consolidation sample disturbance using the *e*-log *P* curve (Silva, 1975), was applied to these samples. Most I_D values fall within the range 0.25 to 0.45, which is considered low to moderate disturbance. Bennett et al. (1977) have shown that for sediments with initial porosities of less than 65% the disturbance index technique is biased toward higher I_D values for the same relative amount of disturbance. Thus the disturbance index criterion classifies the most disturbed consolidation sample tested as

[1] *Initial Reports of the Deep Sea Drilling Project*, Volume 66.
[2] Present address: Sandia National Laboratories, Division 4536, Albuquerque, New Mexico.

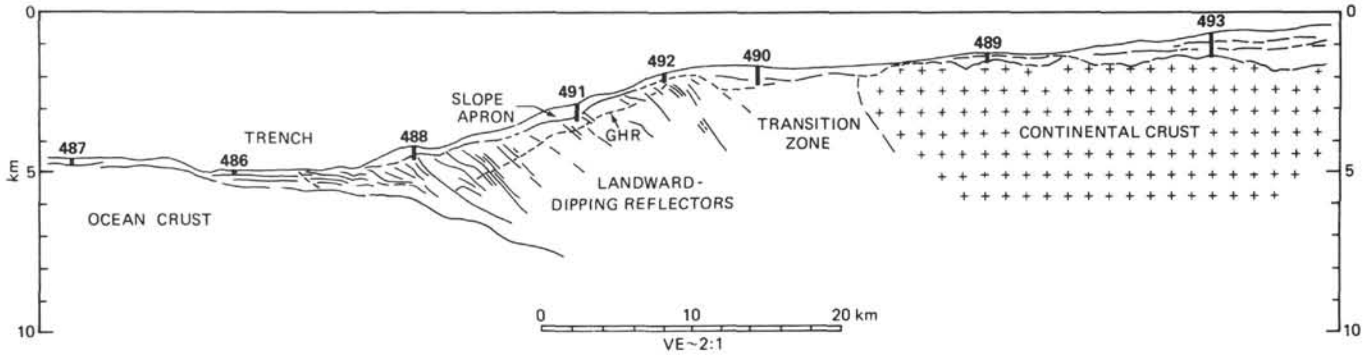

Figure 1. Schematic cross section of Middle America Trench showing appropriate locations of eight drill sites studied.

moderately disturbed. To interpret the state of consolidation, computed preconsolidation pressures were assumed to represent minimum values, which are lower than actual *in situ* preconsolidation values (Schmertmann, 1955).

RESULTS

Site 487

Drilling at Site 487, located on the trench outer slope of the seaward plate (Fig. 1), penetrated 105 meters of Quaternary hemipelagic silty clays overlying 67 meters of upper Miocene to Pliocene brown pelagic clays. Geotechnical analyses of these sediments (Fig. 2) reveal subtle differences corresponding to changes in lithology and/or sedimentation rate.

Water content increases from 50% at the sediment water interface to 58% at 12 meters, then remains fairly constant to 158 meters sub-bottom. Inflections in the water content depth profile at 103 and 134 meters bracket the transition from predominantly hemipelagic Quaternary silty clays to Pliocene–upper Miocene pelagic clays. This transition results in decreased sedimentation rates and changes in dominant lithologic types. Concomitant changes occur for porosity and bulk density; from 80% to 75% and 1.35 Mg/m^3 to 1.44 Mg/m^3 at the surface and 158 meters, respectively.

The lack of significant changes in these properties in the upper 150 meters appears consistent with values reported for pelagic sediments at other sites (Hamilton, 1976). The inflections in the index property gradients at 103 and 134 meters probably reflect *in situ* trends. No apparent increase in core disturbance, either mechanical or gas-related, occurs at these depths.

Compressional velocity increased gradually from 1.45 km/s to 1.54 km/s at 102.5 meters. Below this depth, velocity remains relatively constant. These values are within the expected range for high-porosity clays and silty clays, using the relationships developed by Nafe and Drake (1957) and Cernock (1970).

Shear strength remains relatively constant—15 kPa—to a depth of 40 meters. Values appear to increase gradually at greater depths, exceeding 100 kPa at 112 meters. Scatter in the shear strength profile results from premature failure by cracking and may also reflect zones of disturbance not evident visually. Shear strength, effective overburden pressure ratios ($C_u \cdot P_o'^{-1}$) range from 0.11 at the mudline to 0.20 at 140 meters, indicating that these sediments are underconsolidated according to the range of values (0.2–0.5) suggested for normally consolidated marine clays (Skempton, 1970).

Three consolidation tests (Fig. 3 and Table 1) performed on sediments from this site also show the sediments to be underconsolidated. Problems incurred while loading Sample 487-18-5 and the absence of a well-defined break in slope on the *e*-log *P* curve limit confidence in the preconsolidation pressure determined for this test. These results concur with those expected based on the porosity and water content profiles, and indicate that very little dewatering has occurred within the sediment cored.

Site 488

Site 488 was located approximately 4 km from the trench axis at the base of the trench inner slope. Drilling penetrated 313 meters of middle to upper Quaternary clayey silts, which overlie 115 meters of lower to middle Quaternary clayey silts interbedded with sand. These sands vary in thickness from less than a meter to several meters. Geotechnical analyses (Fig. 4) were limited to the clayey silt sediments penetrated at this site. Attenuation of the sonic signal by gas precluded any compressional sound velocity measurements.

Porosity gradually decreases from near-surface values of 70% to 49% at 210 meters (Fig. 4). From 210 to 235 meters porosity abruptly decreases to 35%, then gradually increases to 45% at 300 meters. Below 300 meters porosity again decreases, although limited core recovery and increasing amounts of scatter due to fissility and variations in silt content have resulted in a poorly defined trend.

Water content and bulk-density depth profiles reveal trends similar to the porosity depth profile trend. Water content decreases gradually (47%–27%) to 210 meters sub-bottom, then abruptly decreases over a 25-meter interval to 14.5% at 235 m. Below 235 meters water content increases (14.5%–33%) to 300 meters, then gradually decreases to 400 meters sub-bottom (33%–15%). Bulk density increases gradually (1.53 Mg/m^3–1.75 Mg/m^3) to 210 meters sub-bottom, then abruptly increases between 210 and 235 meters (1.75 Mg/m^3–2.05 Mg/m^3). A decrease in bulk density (2.05 Mg/m^3–1.88 Mg/m^3) occurs from 235 to 300 meters, then bulk density again increases (1.88 Mg/m^3–1.98 Mg/m^3) to a sub-bottom depth of 400 meters.

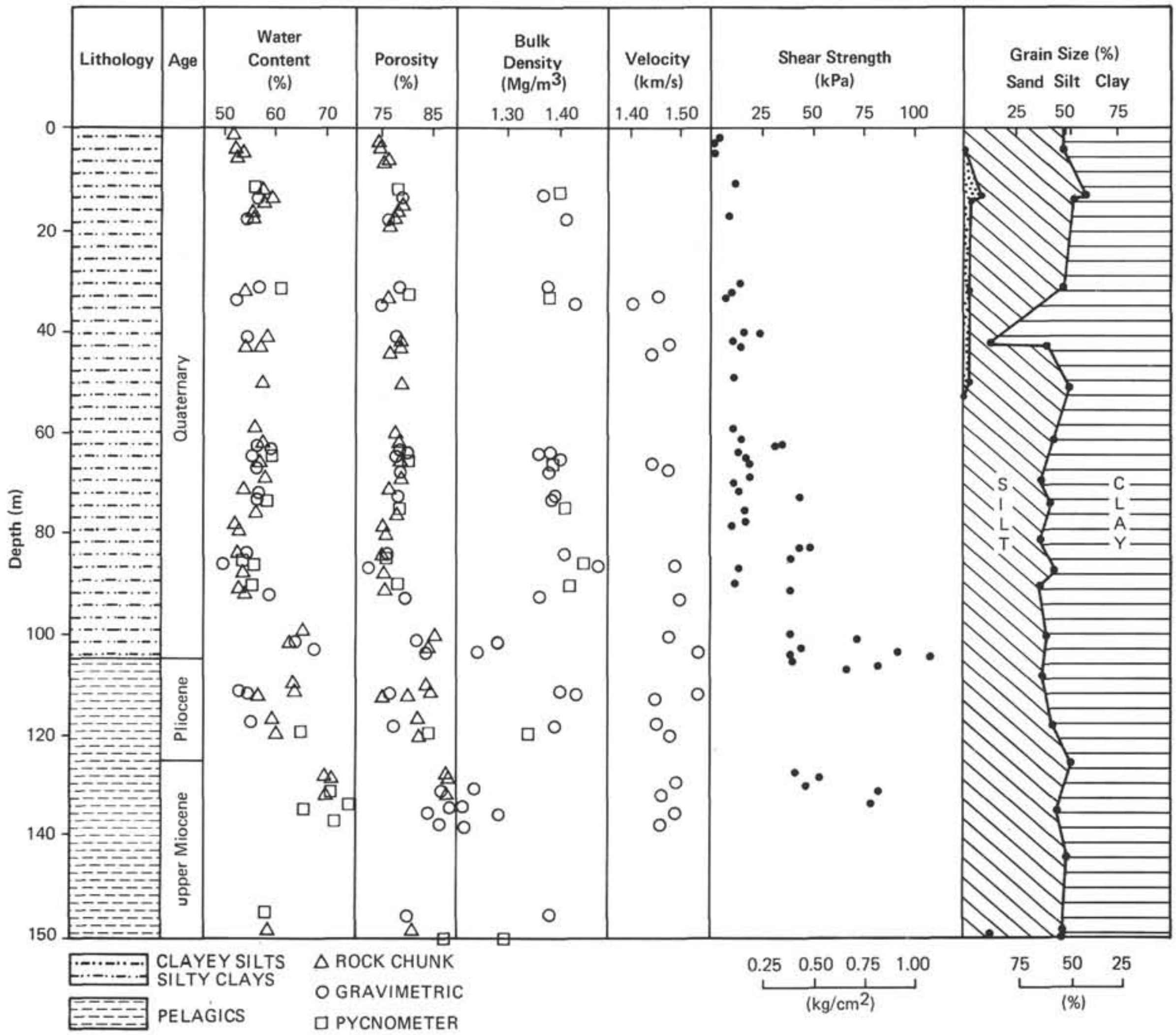

Figure 2. Geotechnical property summary profiles, Site 487.

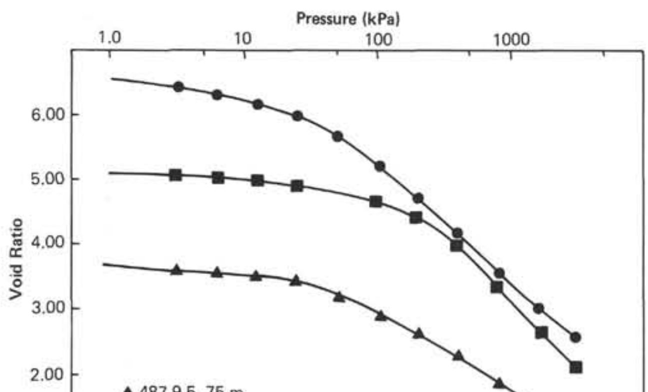

Figure 3. Void ratio versus logarithm of pressure curves e-log P for Site 487 samples.

Shear strength (Fig. 4) increases uniformly from 4.4 kPa at 3.3 meters to 98 kPa at 202 meters. The scatter on the shear strength profile results from premature failure by cracking and possibly from variations in disturbance not evident visually. Ratios of undrained shear strength to effective overburden pressure $C_u \cdot P_o'^{-1}$ for maximum shear strengths measured at a particular depth gradually decrease from 0.14 at 25 meters to 0.09 at 170 meters. These values are lower than those proposed by Skempton (1970) for normally consolidated marine clays and suggest that these sediments are underconsolidated.

Ten consolidation tests were performed on Site 488 sediments (Fig. 5; Table 2). Test results indicate that Sample 488-2-3 (4.0 m) is overconsolidated; remaining inner trench slope samples are underconsolidated.

Underconsolidated sediments at depth agree with predictions based on shear strength data. Overconsolidation ratios (OCR) are fairly consistent below 10 meters sub-bottom (0.20–0.41), except for Sample 488-26-2 (0.04; 238 m). These constant OCR values indicate that sediments are not becoming more underconsolidated with depth, as was evident within the Japan Trench complex (Shephard and Bryant, 1980), but that excess pore pressures associated with these sediments are dissipating to a certain degree commensurate with accumulating overburden. The low OCR value for Sample 488-

Table 1. Consolidation test results and geotechnical properties of samples tested from Site 487.

Core/Section	Depth below Seafloor (m)	Bulk Density (Mg/m³)	Porosity (%)	Water Content (%)	Void Ratio	Effective Overburden Pressure (kPa)	Preconsolidation Pressure (kPa)	Overconsolidation Ratio
Hole 487								
9-5	75	1.41	78.56	58.86	3.67	287	70	0.24
14-3	119	1.34	84.19	64.16	5.33	440	310	0.71
18-5	160	1.29	86.67	68.44	6.50	559	60	0.11

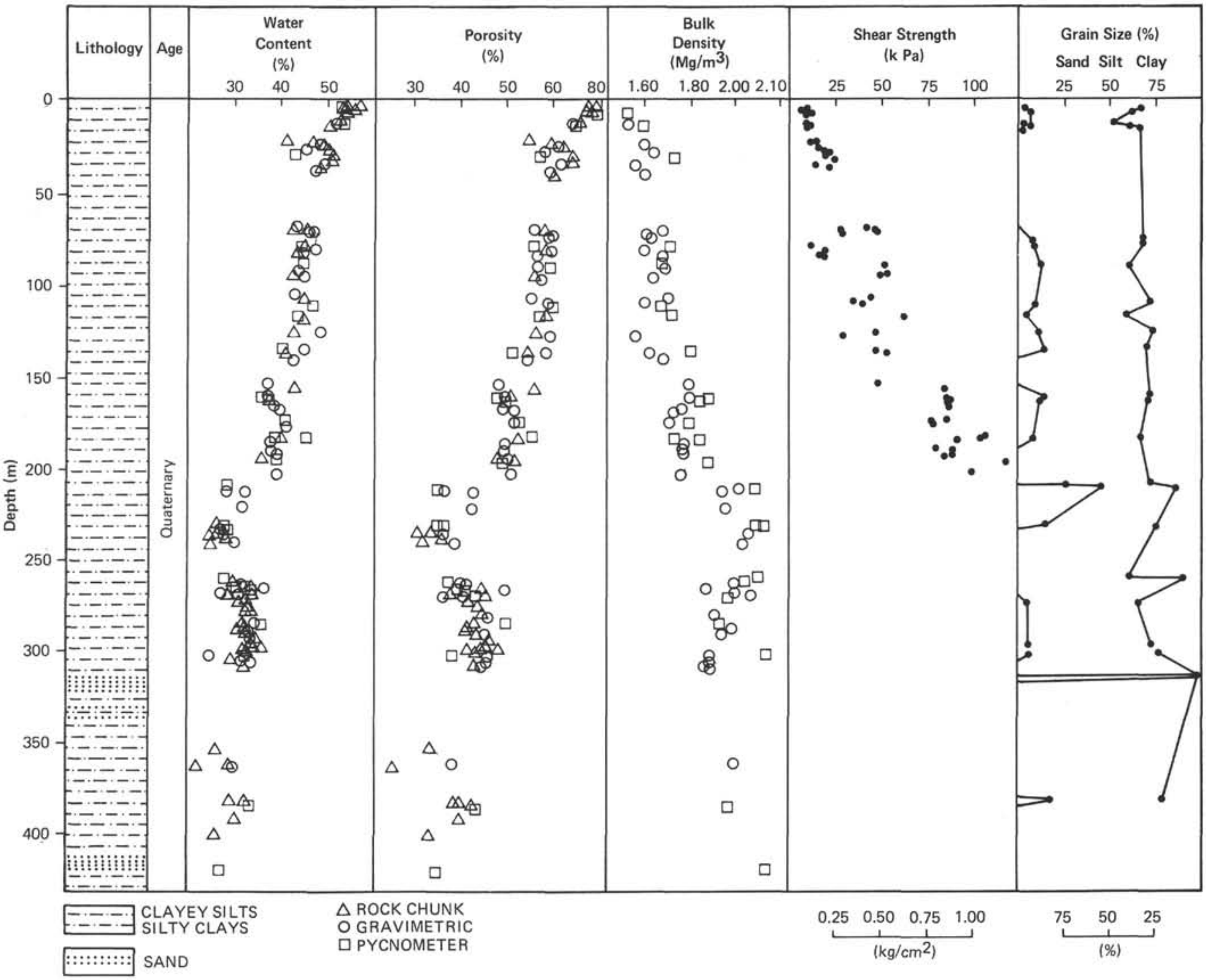

Figure 4. Geotechnical property summary profiles, Site 488.

26-2 appears related to increased sediment deformation evident as truncated bedding, variable bedding attitudes, and inclined fractures in sediments above and below the consolidation sample. An increase in fine sand and a disrupted, chaotic clay fabric which appears to have formed *in situ* may also contribute to the anomalously low OCR value.

No anomalies in the geotechnical properties are evident in the upper 200 meters, which can be correlated with the thrust fault evident on the site survey seismic reflection profiles (Shipley, this volume). However, Shipley has identified a nearly horizontal coherent reflection occurring very near the depth of the geotechnical properties anomaly at 235 meters. Cores obtained through this zone show steeply dipping and truncated beds as well as inclined fractures, which suggest deformation resulting from tectonic or mass movement processes. Extrapolation of the bulk properties trend

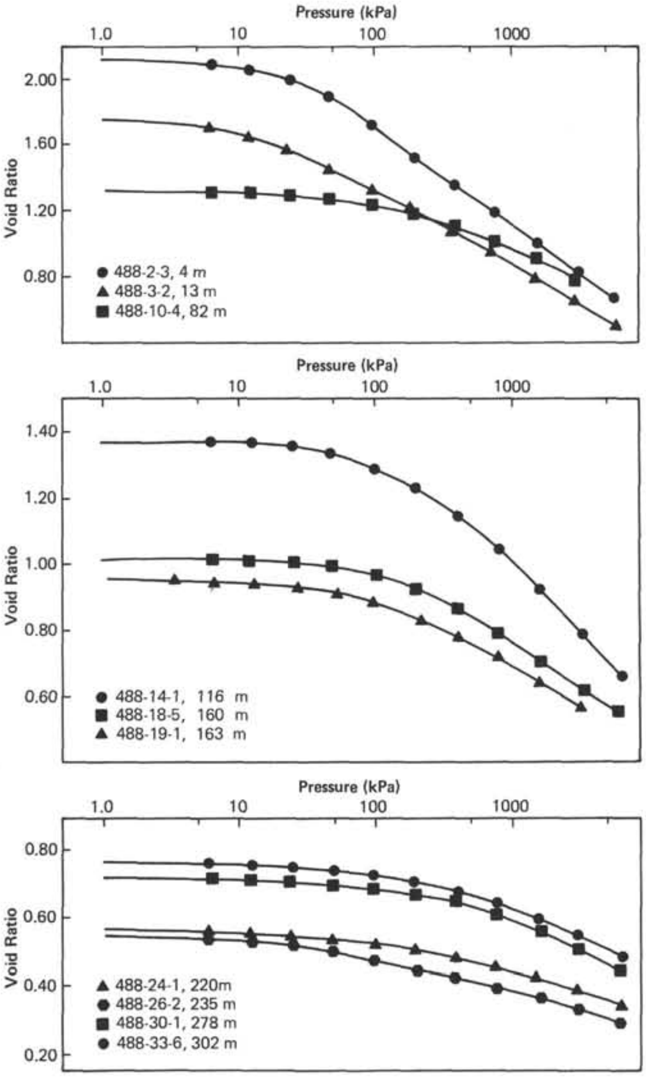

Figure 5. Void ratio versus logarithm of pressure curves, e-log P for Site 488 samples.

developed in the upper 200 meters to below the anomalous zone results in values of porosity, water content, and bulk density very close to those values actually measured. Woodbury et al. (1978) studied a large sediment mass in the Gulf of Mexico, displaying very similar geotechnical property trends with depth, which they interpreted as a major slump block.

Transmission electron micrographs of ultrathin sections (≈800Å–1000Å thick) from sediments above, below, and within the zone of deformation reveal definite changes in clay fabric (Fig. 6). Micrographs of Sample 488-20-1 (180 m) show a preferentially oriented clay fabric consisting of domains of clay particles, some of which appear oblique to the preferred direction of orientation. This type of fabric probably results from natural consolidation processes due to increasing overburden pressure. Micrographs of Samples 488-24-1 and 488-26-2 (220 and 235 m, respectively) reveal a different clay fabric. Sample 488-24-1 clay fabric consists of well-defined domains which appear randomly oriented. Sample 488-26-2 clay fabric appears more disrupted with fewer well-defined domains and an increase in electron dense particles. Micrographs of Sample 42-6 (385 m), located below the zone of deformation, show well-defined and highly oriented domains probably indicative of normal gravitational compaction processes.

Deformation of Site 488 sediments evident visually, evident in the geotechnical property profiles, and evident in electron micrographs of ultrathin sections is most pervasive between 210 and 250 meters sub-bottom. This zone of deformation appears related to the convergence process either directly by the deformation of lower slope sediments during accretion and subsequent uplift of underlying trench sediments or indirectly by inducing excess pore pressures and oversteepened slopes resulting in mass movement. Regardless of the mechanism, this zone represents one type of soft sediment deformation occurring on the lower trench inner slope. An increase in the silt and fine sand size fractions may also have some effect on the geotechnical properties and clay fabric of these sediments.

Site 489

Drilling at Site 489, located over continental crust, penetrated 5.5 meters of Quaternary clayey silts unconformably overlying 295 meters of Miocene clayey silts. Geotechnical analyses (Figure 7) reveal subtle changes in the index property gradients, particularly below 50

Table 2. Consolidation test results and geotechnical properties of samples tested from Site 488.

Core/Section	Depth below Seafloor (m)	Bulk Density (Mg/m^3)	Porosity (%)	Water Content (%)	Void Ratio	Effective Overburden Pressure (kPa)	Preconsolidation Pressure (kPa)	Overconsolidation Ratio
Hole 488								
2-3	4	1.53	68.84	45.77	2.21	22	50	2.24
3-2	13	1.59	65.36	41.65	1.89	71	20	0.28
10-4	82	1.71	56.28	34.43	1.29	483	130	0.27
14-1	116	1.72	57.15	33.55	1.33	641	260	0.41
18-5	160	1.88	48.09	25.86	0.93	930	180	0.19
19-1	163	1.84	49.97	27.48	1.00	953	200	0.21
24-1	220	2.14	34.84	16.94	0.54	1302	400	0.31
26-2	235	2.08	35.89	17.97	0.56	1516	50	0.03
30-1	278	1.99	40.95	21.51	0.69	1853	600	0.32
33-6	302	1.96	42.90	22.00	0.75	2196	650	0.30

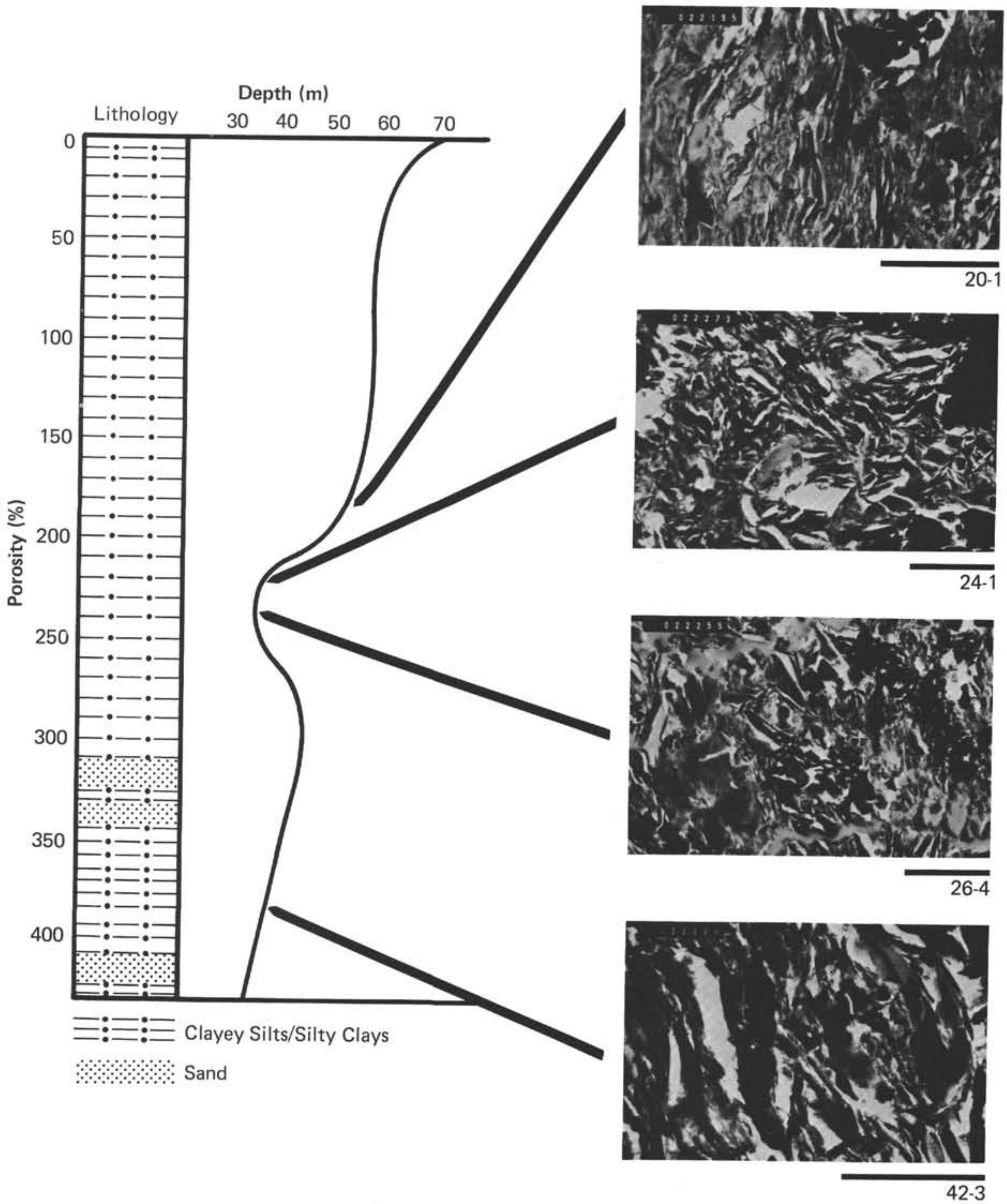

Figure 6. Transmission electron photomicrographs of ultrathin sections from Site 488 Samples 488-20-1, 488-24-1, 488-26-4, and 488-42-3 located above, within, and below the zone of deformation, respectively. Note high degree of preferential grain orientation in samples above and below zone and disrupted unoriented grain relationships from within zone of deformation. (Scale bar = 1 μm.)

meters. Scatter in these profiles results from varying degrees of lithification, evident visually, and may be attributed to differences in the amount of carbonate precipitation within the voids and fluctuations in silt clay percentages.

Porosity and water content display similar trends, decreasing from 61% and 34% at 1.5 meters to 30% and 13% at 285 meters, respectively. Bulk density increases from 1.70 Mg/m^3 at 3.15 meters to 2.16 Mg/m^3 at 289 meters and displays abundant scatter for the reasons just mentioned.

Compressional sound velocity increases from 1.60 km/s at 12 meters to 1.90 km/s at 237 meters. These values are variable with depth and appear lower than

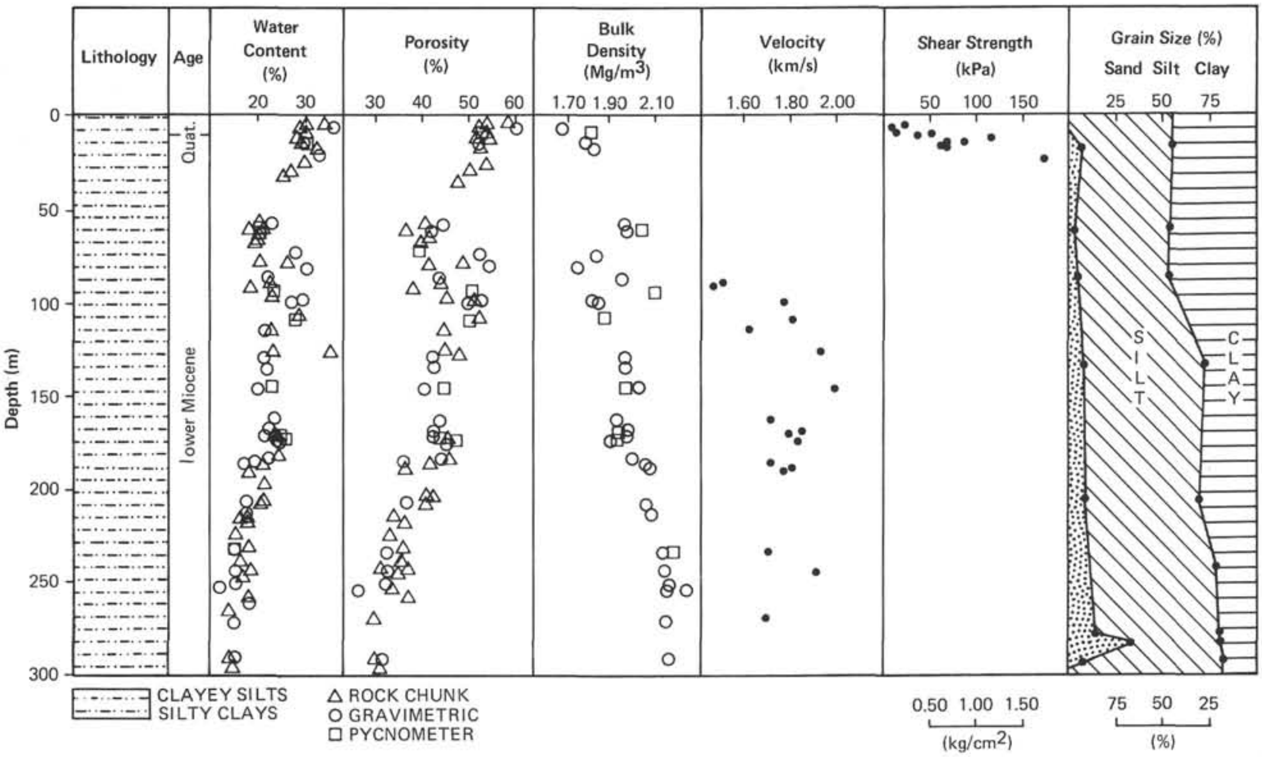

Figure 7. Geotechnical property summary profiles, Site 489.

those obtained from velocity analyses of multichannel seismic data (2.0 km/s average).

Shear strength increases rapidly from 11.7 kPa at 3.75 meters to 173.8 kPa at 22 meters, below which failure by cracking precluded further measurements. $C_u \cdot P_o'^{-1}$ ratios computed using maximum values of shear strength at a particular depth exceed 1.0, suggesting these sediments are underconsolidated.

Two consolidation tests, performed on sediments obtained from 13.50 and 61.50 meters (Fig. 8; Table 3), show these sediments to be normally to overconsolidated. Overconsolidation ratios for these samples are 1.34 for 489A-2-6 (13.50 m) and 1.03 for 489A-4-4 (61.50 m).

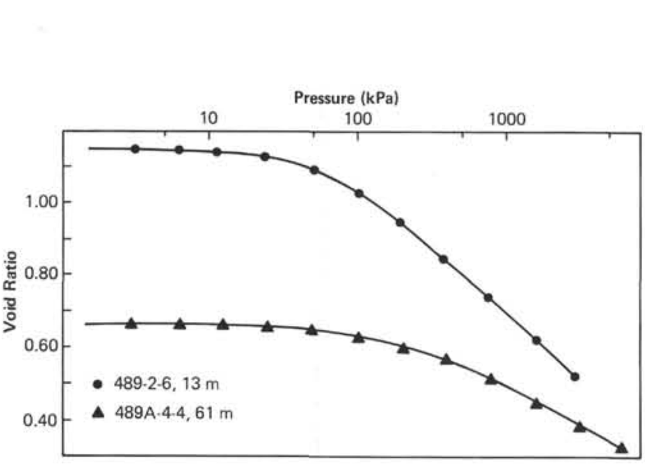

Figure 8. Void ratio versus logarithm of pressure curves *e*-log *P* for Site 489 samples.

Site 490

Site 490 is located in the transition zone between continental crust and landward-dipping reflectors (Fig. 1). Drilling penetrated 142 meters of Quaternary clayey silts overlying 346 meters of Pliocene to upper Miocene silty clays. Geotechnical analyses (Fig. 9) show rapid changes in these properties from 0 to 50 meters, a gradual uniform change from 50 to 400 meters corresponding to the transformation from soft sediment to siltstone, and below 400 meters a small but significant change possibly reflecting an increase in deformation at this depth.

Porosity and water content decrease gradually from 68% to 48% at 2.3 meters to 35% and 16% at 540 meters, respectively. Bulk density increases from 1.53 Mg/m^3 at 2.3 meters to 2.11 Mg/m^3 at 540 meters.

Compressional sound velocity measurements were limited to sediments cored below 350 meters because of attenuation due to gas. Those velocities measured range from 1.71 km/s to maximum values of 1.88 km/s. These values agree very well with those derived from multichannel seismic reflection data, 1.81 km/s (Shipley, this volume) and those expected on the basis of porosity velocity relationships developed by Nafe and Drake (1957).

Shear strength increases from 11.7 kPa at 1.95 meters to 110 kPa at 106.5 meters. Scatter in the shear strength profile results from premature failure by cracking, especially below 50 meters, and possible variations in disturbance. $C_u \cdot P_o'^{-1}$ ratios, computed using maximum shear strength values with depth, decrease gradually from 0.51 at 10 meters to 0.33 at 60 meters, indicating these sediments are normally consolidated.

Table 3. Consolidation test results and geotechnical properties of samples tested from Site 489.

Core/Section	Depth below Seafloor (m)	Bulk Density (Mg/m^3)	Porosity (%)	Water Content (%)	Void Ratio	Effective Overburden Pressure (kPa)	Preconsolidation Pressure (kPa)	Overconsolidation Ratio
Hole 489								
2-6	13	1.82	53.80	30.70	1.17	97	130	1.34
Hole 489A								
4-4	61	2.05	39.58	19.22	0.66	520	507	1.03

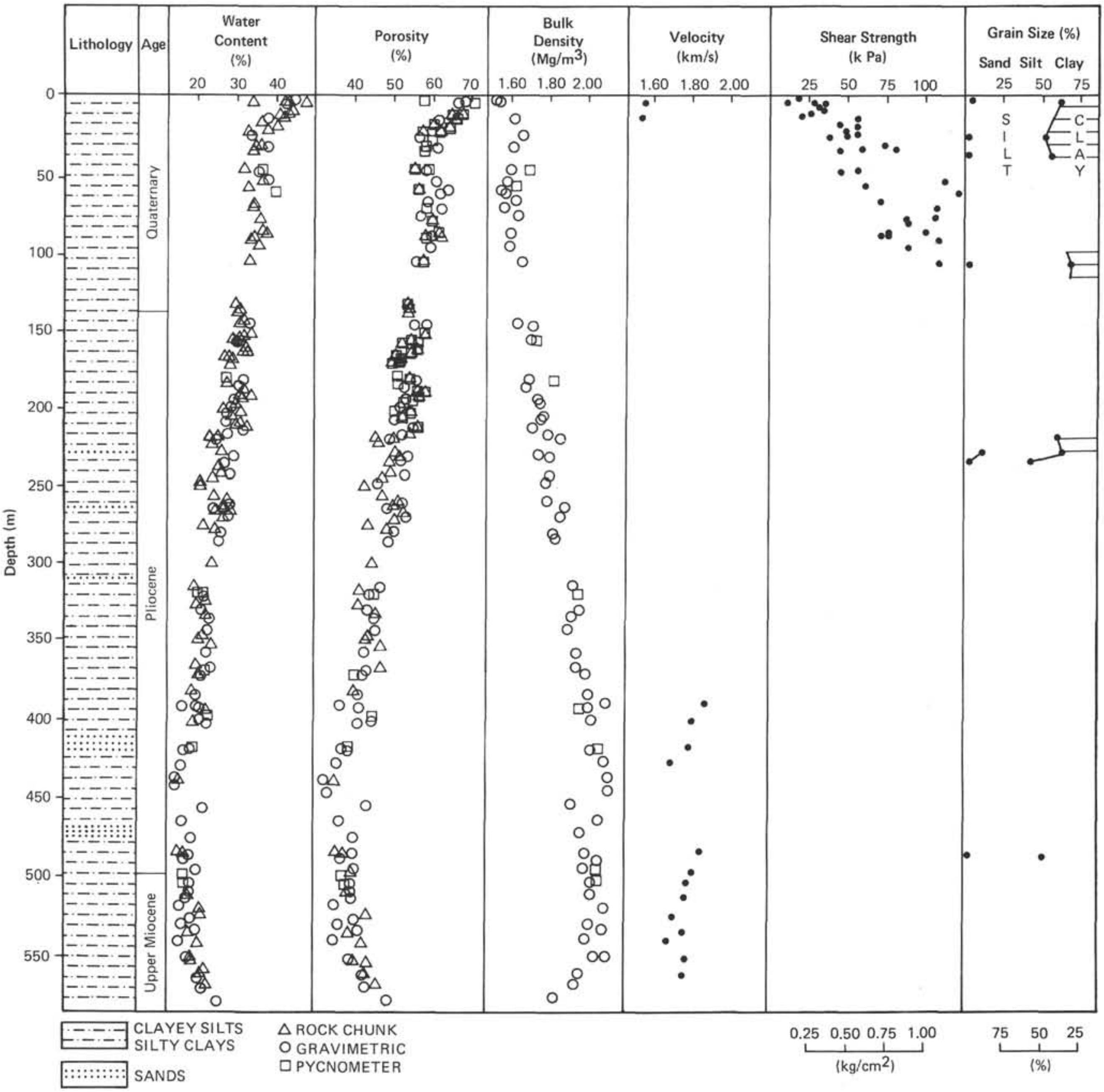

Figure 9. Geotechnical property summary profiles, Site 490.

Site 491

Drilling in the middle trench inner slope (Fig. 1), Site 491 penetrated 542 meters of Quaternary and Pliocene silty clays. Geotechnical analyses (Fig. 10) reveal uniformly gradational changes to 410 meters sub-bottom, below which there is an apparent increase in the amount of induration. Attenuation due to gas prevented compressional sound velocity measurements.

Porosity and water content decrease from 66% and 44% at 0.50 meters to 33% and 15% at 525 meters, respectively. Both porosity and water content decrease more rapidly below 410 meters. Bulk density increases from 1.58 Mg/m^3 at 6.60 meters to 2.07 Mg/m^3 at 520 meters. This break in geotechnical properties below 410 meters corresponds approximately to lithologic Unit 3, a zone of increasing sand content with depth, implying that some of this change results from lithologic variation.

Shear strength increases regularly from 13.5 kPa at 0.50 meters to 122.5 kPa at 69 meters. $C_u \cdot P_o'^{-1}$ ratios average 0.27 to a depth of 70 meters, suggesting these sediments fall within the range of values suggested by Skempton (0.2–0.5, 1970) for normally consolidated sediments.

Four consolidation tests performed on Site 491 sediments (Fig. 11; Table 4) indicate Samples 491-2-4 (15.50 m) and 491-6-3 (52.00 m) are normally to slightly overconsolidated (OCR = 1.32 and 0.99, respectively), whereas Samples 491-17-5 (150.50 m) and 491-25-5

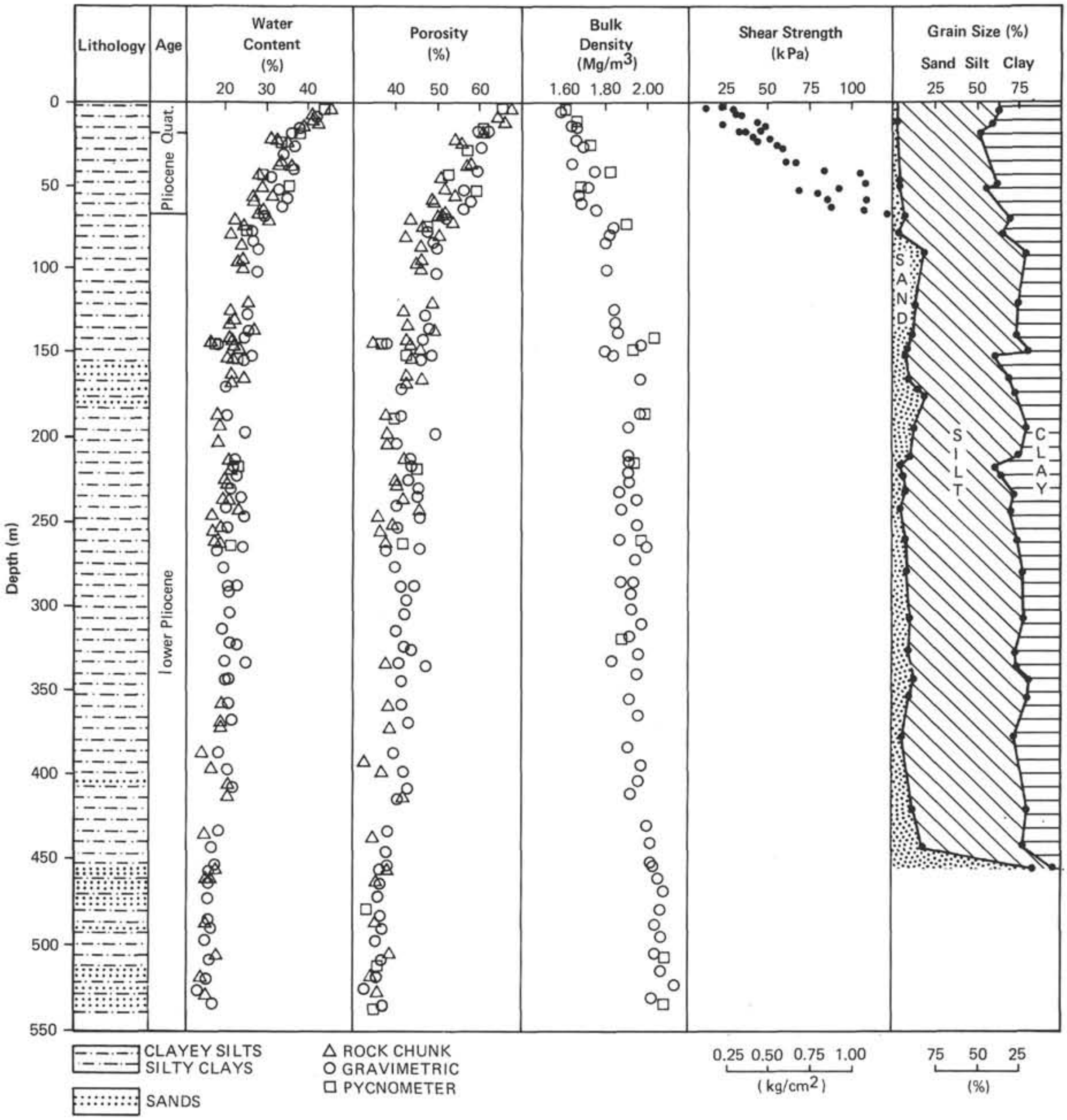

Figure 10. Geotechnical property summary profiles, Site 491.

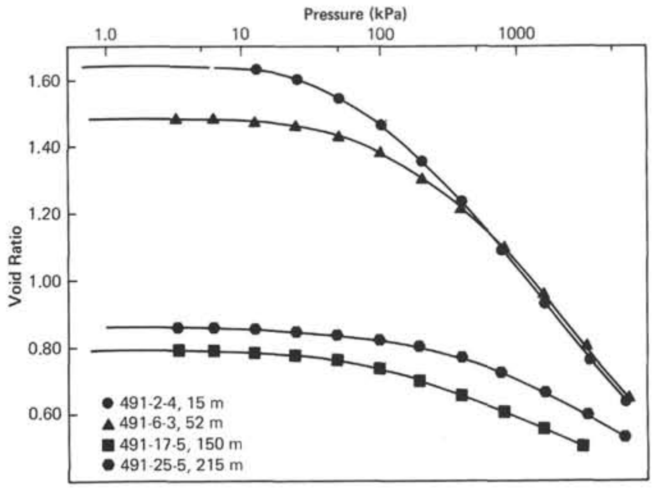

Figure 11. Void ratio versus logarithm of pressure curves *e*-log *P* for Site 491 samples.

(215.50 m) are underconsolidated (OCR = 0.13 and 0.39, respectively). Test results from the two shallowest samples agree very well with the consolidation state predicted on the basis of shear strength. Overconsolidation ratios for the deeper samples are within the range of OCR values developed from test results on underconsolidated Site 488 samples.

Site 492

Drilling at Site 492, located seaward of the trench slope break on the trench inner slope (Fig. 1), penetrated 247 meters of Quaternary to upper Miocene clayey silts overlying 43 meters of Miocene clayey silts interbedded with sand. Sands varied in thickness from less than 1 meter to several meters. General geotechnical results (Fig. 12) from Site 492, Holes 492, 492A, and 492B, will be discussed jointly. In addition, a comparison of results utilizing standard rotary and hydraulic piston cores will be presented.

Gas expansion and related core disturbance greatly influenced the index properties of Hole 492 sediments, particularly between 125 and 200 meters. Signal attenuation due to gas precluded compressional sound velocity measurements. Porosity decreases from 66% at 8.0 meters to 49% at 110 meters, below which porosity increases to 54% at 160 meters, then decreases to a minimum of 34% at 286 meters. Water content decreases from 35% at 0.50 meters to 26% at 110 meters. Below 110 meters water content increases to 32% at 150 meters, then decreases to 18% at 286 meters. Bulk density displays the inverse trend, gradually increasing from 1.57 Mg/m^3 to 1.86 Mg/m^3 at 80 meters and 110 meters, respectively. Bulk density then decreases to 1.74 Mg/m^3 at 160 meters and finally increases to a maximum of 1.96 Mg/m^3 at 286 meters.

Shear strength increases from 5.9 kPa at 1.40 meters to a maximum of 119.6 kPa at 48 meters (Fig. 13). Scatter in this profile results from variations in drilling disturbance and in silt clay ratios. $C_u \cdot P_o'^{-1}$ ratios, determined using a best fit line through Site 492 shear strength data, increase gradually from 0.65 at 10 meters to 0.85 at 40 meters. These values indicate sediments in the upper 40 meters to be normal to overconsolidated using the range of values presented by Skempton (1970).

Sixteen consolidation tests performed on Site 492 sediments (Figs. 14, 15, 16; Table 5) show normal to overconsolidated sediments in the upper 135 meters, below which test results indicate underconsolidation. Overconsolidation ratios for all of Hole 492A samples are greater than 2.0 and increase with depth to a maximum of 6.20 at 26 meters. Ratios determined for Hole 492 samples within the upper 30 meters vary between 1.67 and 2.77 and also indicate overconsolidated sediments. Below 30 meters, however, OCR values vary from 0.303 at 36.50 meters to 5.304 at 104.50 meters. Deeper samples, 492-26-5 and 492-30-1 (239.00 m and 266.50 m, respectively), are very underconsolidated with OCR values of 0.20 and 0.08, respectively.

Comparison of bulk property results from Holes 492 and 492A (Fig. 13) reveals only subtle variations in porosity, water content, and bulk density between rotary drilled and hydraulic piston cored samples. Although visual observations of these cores failed to resolve any increase in disturbance due to the rotary drilling technique, shear strength measurements revealed interesting differences between samples at similar depths obtained by both coring techniques. Shear strengths of rotary drilled samples display much more scatter, particularly below 20 meters, than do the samples obtained with the hydraulic piston corer. This suggests that, although disturbance caused by rotary drilling may not be visually evident in relatively high shear strength sediments, it nevertheless causes partial remolding and a decrease in cohesion. OCR values are significantly higher for hydraulic piston cored samples than for rotary drilled samples; this also suggests partial remold-

Table 4. Consolidation test results and geotechnical properties of samples tested from Site 491.

Core/Section	Depth below Seafloor (m)	Bulk Density (Mg/m^3)	Porosity (%)	Water Content (%)	Void Ratio	Effective Overburden Pressure (kPa)	Preconsolidation Pressure (kPa)	Overconsolidation Ratio
Hole 491								
2-4	15	1.65	61.40	37.46	1.59	91	120	1.32
6-3	52	1.69	58.55	35.42	1.41	355	350	0.99
17-5	150	1.93	43.69	22.90	0.78	1189	150	0.13
22-5	215	1.93	45.45	23.72	0.83	1789	700	0.39

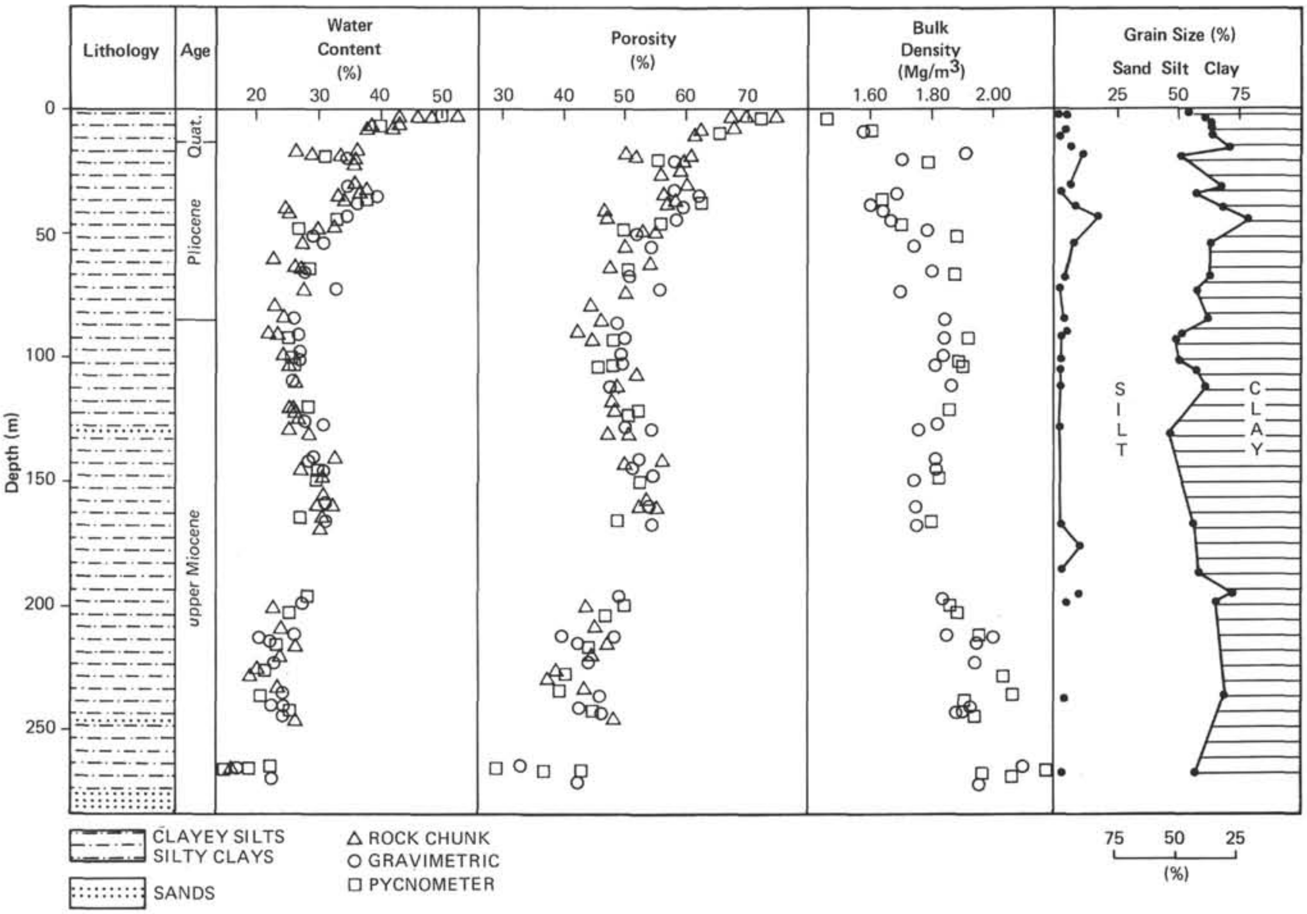

Figure 12. Geotechnical property summary profiles, Site 492.

ing, possibly on a grain-to-grain scale, which may be evident in clay fabric and transmission electron microscopy techniques.

Shear strength and consolidation test results indicate the value of the hydraulic piston corer to any detailed geotechnical program. In sediments where shear strengths are more typical of normal or underconsolidated sediments (< 100 kPa) at depth, differences in geotechnical properties may be even more substantial.

Problems with the hydraulic piston corer did occur, however, when shear strengths exceeded 75 kPa. "Flow in" evident as smeared vertical laminations as well as collapsed core liners resulted in low recovery of good quality sediment, severely limiting the usefulness of the corer.

Site 493

Site 493, the most landward of all sites drilled (Fig. 1), penetrated 50 meters of Quaternary clayey silts, overlying 310 meters of Pliocene and Miocene clayey silts grading into 287 meters of lower Miocene silty sands. This overall transgressive sequence displays a gradual change in geotechnical properties with depth (Fig. 17).

Porosity decreases gradually from 62.5% at 40 meters to 48% at 360 meters. Between 360 and 365 meters a 5% decrease in porosity to 43% occurs. Below 365 meters porosity gradually decreases to 32% at 570 meters. Scatter in the porosity depth profile results from variations in sand-silt-clay ratios, gas expansion, and sediment spalling during volume measurements. Water content displays a similar trend, decreasing from 44% at 43 meters to 27% at 360 m. From 360 to 435 meters water content remains relatively constant—24%—then decreases between 435 and 579 meters to 19%. Bulk density is variable in the upper 365 meters, increasing from 1.60 Mg/m^3 at 40 meters to 1.79 Mg/m^3 at 360 meters. Below 360 meters density abruptly increases, to 1.95 Mg/m^3 at 365 meters, then gradually continues to increase, to 2.10 Mg/m^3 at 465 meters. Below 465 meters bulk density remains relatively constant, averaging 2.07 Mg/m^3. Significant changes in porosity and bulk density occur between 360 and 365 meters. These changes correspond directly with a Miocene unconformity at this depth, which probably represents an erosional rather than a nondepositional event.

Shear strength increased from 17 kPa at 12.45 meters to 121 kPa at 127 meters. Scatter in the shear strength profile results from variations in silt-clay ratios and core disturbance. $C_u \cdot P_o'^{-1}$ ratios determined using maximum shear strengths for a particular depth average 0.20, which is the lower limit of the range of values given by Skempton (1970) for normally consolidated clays.

Three consolidation tests show these sediments are underconsolidated (Fig. 18; Table 6), with OCR values falling within the range of those from other sites.

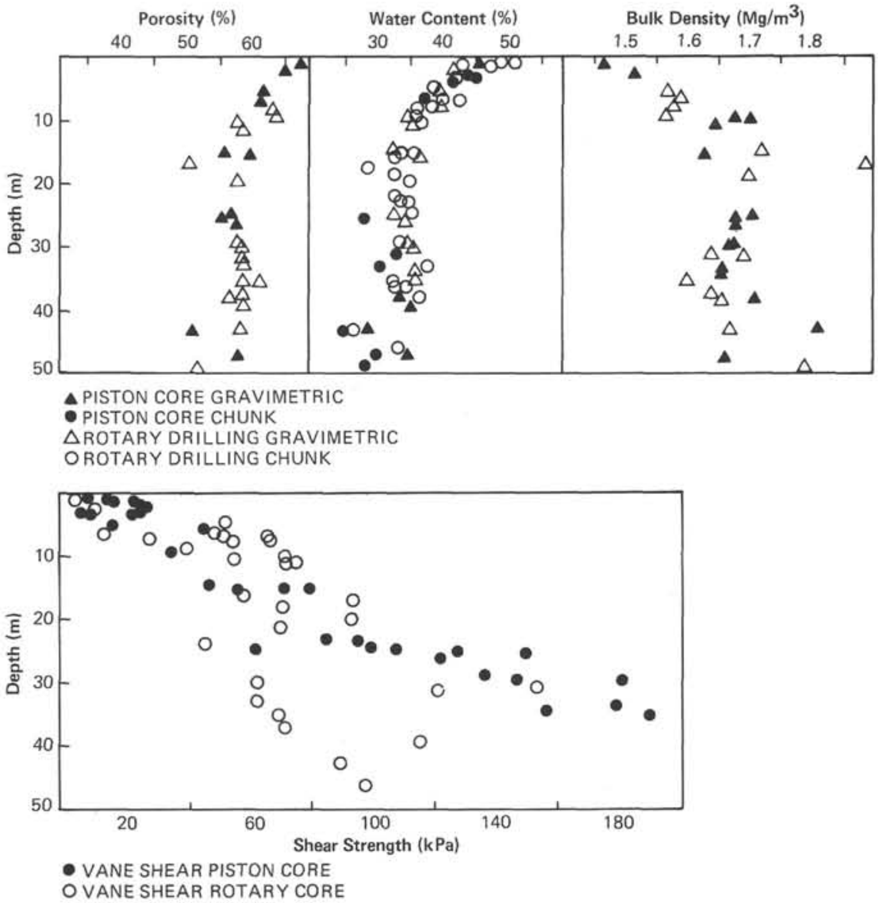

Figure 13. Geotechnical property profiles comparing sediments cored by rotary drilling and hydraulic piston corer techniques. Note similarity in index property trends with depth and increased scatter in sediment shear strengths from rotary drilled samples.

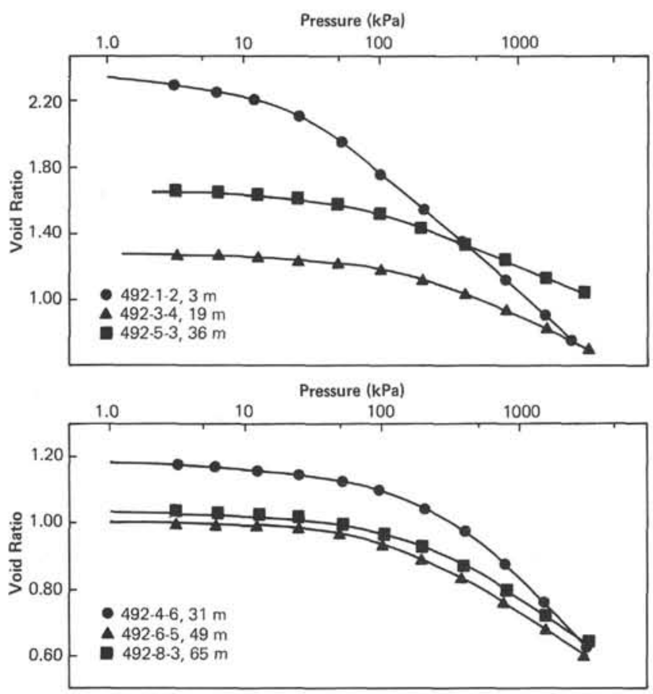

Figure 14. Void ratio versus logarithm of pressure curves e-log P for Samples 492-1-2, 492-3-4, 492-4-6, 492-5-3, 492-6-5, and 492-8-3.

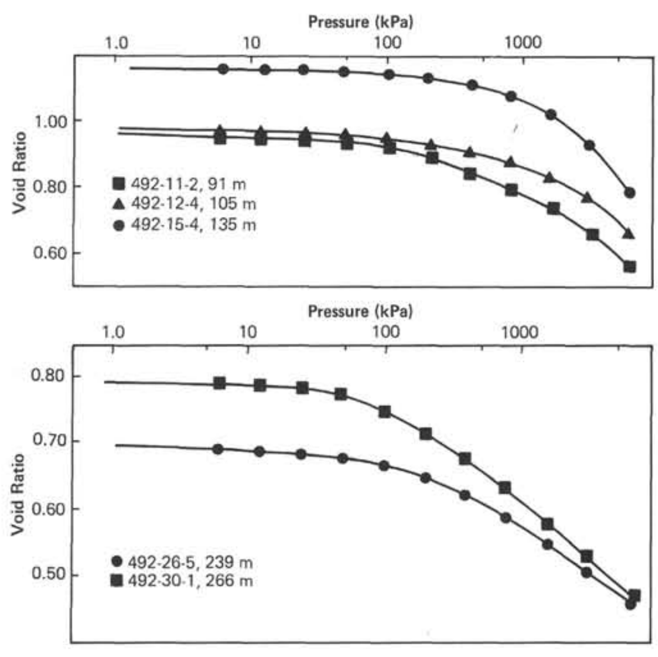

Figure 15. Void ratio versus logarithm of pressure curves e-log P for Samples 492-11-2, 492-12-4, 492-15-4, 492-26-5, and 492-30-1.

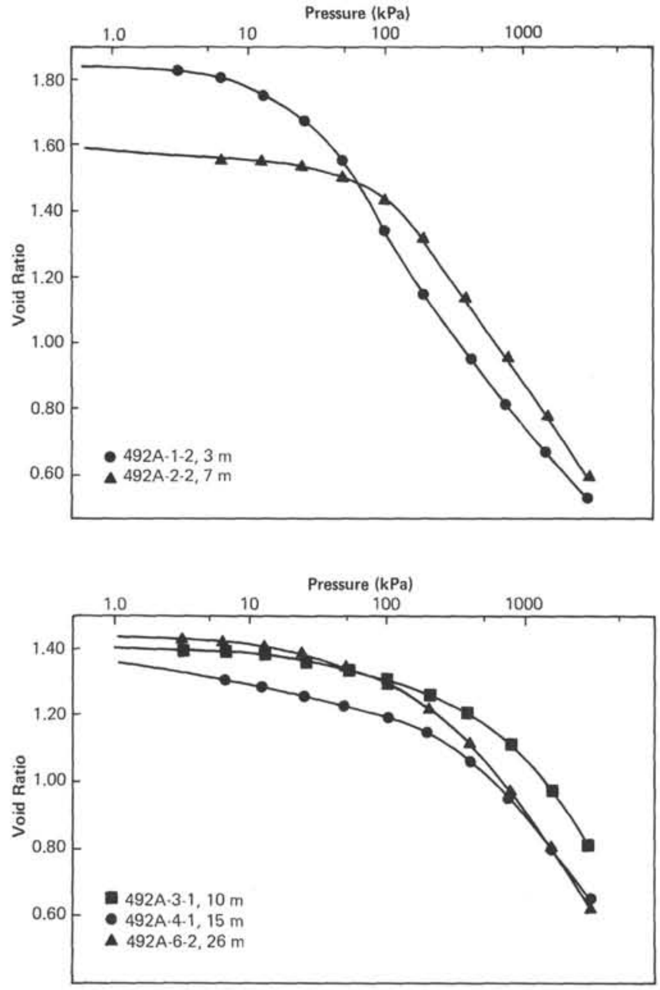

Figure 16. Void ratio versus logarithm of pressure curves *e*-log *P* for Hole 492A samples.

DISCUSSION

The state of consolidation of Middle America Trench sediments appears quite variable. Consolidation test results indicate that sediments tested at Sites 487, 488, and 493 are underconsolidated, whereas sediments tested at Sites 489 and 492 are normal to overconsolidated. Normally consolidated near-surface sediments from Site 491 become underconsolidated with increasing depth.

Underconsolidated sediments result from factors which decrease the effective stress by creating excess porewater pressures. Mechanisms resulting in underconsolidation include (1) rapid sediment accumulation rates, (2) low sediment permeability relative to the length of the drainage path, (3) laterally applied stresses, (4) artesian water pressure or induced water pressure from deeper formations, (5) high concentrations of gas in sediments, and (6) physicochemical interparticle bonding and cementation. Sample disturbance may decrease the preconsolidation pressure sufficiently to result in "apparent" underconsolidation.

Site 487 geotechnical properties display only subtle changes with increasing depth of burial. This indicates that limited dewatering occurs in response to accumulating overburden after initial deposition. Slow accumulation of pelagic clays may result in the development of cohesive interparticle bonds (Hamilton, 1964) which inhibit dewatering resulting in underconsolidated, high porosity, low bulk density sediments at depth.

The response of these high water content sediments ($>50\%$ water by weight) to the rapidly applied overburden as they descend the outer trench slope and under the lower trench inner slope may have important implications concerning lower slope deformation and accretion-subduction processes. In laboratory one-dimensional consolidation tests the sediment structure of pelagic clays readily collapses under a critical load (Mitchell, 1976). This collapse results in a well-defined break in slope on the *e*-log *P* curve which is best illustrated on the *e*-log *P* curve of Sample 487-14-3 (Fig. 2). Although greatly simplified, a similar response occurring while these sediments are descending under the lower trench inner slope could release large quantities of water, thereby causing abnormal pressures. Conversely, if the pelagic sediment structure does not collapse under some critical overburden pressure the pelagic sediment should become abnormally pressured. In areas of high convergence rates, these sediments would be carried into the subduction zone and rapidly loaded under an existing overburden at a rate which may not allow dissipation of excess porewater pressures. Increased deformation within the lower trench slope could result from either mechanism.

Underconsolidated Site 488 sediments accumulated at rates in excess of 380 m/m.y. in the upper 210 meters sub-bottom, below which accumulation rates exceeded 200 m/m.y. When these values are corrected for compaction they exceed 500 m/m.y. (Shephard and MacMillan, this volume) and are of sufficient magnitude to cause underconsolidation where permeabilities are less than 10^{-7} cm/s (Bredehoft and Hanshaw, 1968). Permeabilities of Site 488 sediments fall within the range of 10^{-7} cm/s to 10^{-9} cm/s. Excess pore pressures in subduction complexes have been attributed to laterally applied stresses (Hottman and Smith, 1978). Folding and faulting of lower slope and trench sediments, evident on high resolution and multichannel seismic profiles near Site 488, indicate lateral stresses may be very important in this region. Induced pore pressures from deeper formations may also contribute to the state of underconsolidation. *E*-log *P* curves of closely spaced samples from different cores at Site 488 (cf. Samples 488-18-5 and 488-19-1, and Samples 488-30-1 and 488-33-6, Fig. 5) show many similar characteristics. This improves the reliability of the test results and indicates these results are indicative of *in situ* conditions.

Hamilton (1964) suggests that any factor or combination of factors which result in unusual sediment strength will produce the effect of overconsolidation. Factors most important to this investigation include (1) slow rates of sediment accumulation, (2) removal of previ-

Table 5. Consolidation test results and geotechnical properties of samples tested from Site 492.

Core/Section	Depth below Seafloor (m)	Bulk Density (Mg/m^3)	Porosity (%)	Water Content (%)	Void Ratio	Effective Overburden Pressure (kPa)	Preconsolidation Pressure (kPa)	Overconsolidation Ratio
Hole 492								
1-2	3	1.46	72.04	50.20	2.58	16	35	2.23
3-4	19	1.79	55.76	31.40	1.26	179	300	1.67
4-6	31	1.73	57.20	33.70	1.34	199	550	2.77
5-3	36	1.64	62.23	37.03	1.65	231	90	0.39
6-5	49	1.89	49.18	26.90	0.97	319	160	0.50
8-3	65	1.88	50.37	28.50	1.02	439	280	0.64
11-2	91	1.92	47.43	25.14	0.90	640	300	0.47
12-4	105	1.90	47.50	25.94	0.91	754	4000	5.30
15-4	135	1.80	53.50	30.51	1.15	1002	2100	2.10
26-5	239	2.06	39.00	20.00	0.64	1777	180	0.09
30-1	266	1.98	42.82	21.60	0.75	2041	350	0.20
Hole 492A								
1-2	3	1.55	67.21	44.54	2.05	16	35	2.23
2-2	7	1.61	63.82	40.40	1.76	39	140	3.60
3-1	10	1.64	61.73	38.30	1.61	60	300	5.00
4-1	15	1.73	59.41	35.53	1.46	92	420	4.57
6-2	26	1.72	57.81	34.85	1.37	171	1060	6.22

ously applied overburden by gravity driven mass movement mechanisms, (3) great age, and (4) tectonic induced overpressures. In addition, near-surface sediments (Sample 488-2-3, 4.0 m) may display an "apparent" overconsolidation owing to interparticle cohesion at the time of deposition being greater than the pressure resulting from accumulated overburden.

Overconsolidation ratios slightly in excess of 1.0 and $C_u \cdot P_o'^{-1}$ ratios of 1.0 indicate Site 489 Miocene sediments are overconsolidated, although the exact cause and degree of overconsolidation is unclear. A Miocene-Quaternary unconformity penetrated at this site is interpreted as an erosional rather than nondepositional event on the basis of seismic reflection data (see Site 489 summary; this volume). Regression analysis of the shear strength depth profile ($Z = 0.103\ C_u + 2.73$; correlation coefficient 0.898), however, indicates the removal of only 3 to 5 meters of overburden, corroborating the consolidation test results. This would not be sufficient to result in truncated and chaotic reflector configurations suggestive of an erosional unconformity. $C_u \cdot P_o'^{-1}$ values greater than the range suggested by Skempton (1970) for normally consolidated sediments may result from slow sediment accumulation rates (<30 m/m.y.) in conjunction with development of interparticle bonding causing high shear strength at shallow depth.

Several factors may have contributed to the overconsolidated state (OCR $\geq$ 1.0) of Site 492 sediments. This site is located just seaward of the trench slope break, a region actively upbuilding, where deposition and subsequent removal of overburden resulting in overconsolidation are possible. Sands penetrated at the base of Hole 492B indicate original deposition within the trench or lowermost slope where deformation is actively occurring. Low sediment accumulation rates (<40 m/m.y.) and the age (Miocene) of these sediments at shallow depths could also result in overconsolidation. Sediments having OCR values of less than 1 may have been subjected to increased mechanical or gas-related disturbance not evident visually or by radiography.

Site 491 sediments are normally consolidated to a maximum depth of 50 meters, below which they become underconsolidated. Sedimentation rates in the upper 70 meters are very low (<45 m/m.y.) but increase to an average of greater than 900 m/m.y. (uncorrected for compaction) below 150 meters. These extremely high rates of sediment accumulation at depth are responsible for the underconsolidation of the deeper sediments.

Bulk property results indicate that in spite of extreme sedimentation rates Site 491 sediments have dewatered sufficiently to result in porosities approximately equal to those of sediments penetrated at similar depths at Sites 488 and 492. Tectonic-related deformation and dewatering may be partially responsible for these low bulk property values.

EFFECTS OF CONVERGENCE ON GEOTECHNICAL PROPERTIES

Prior to the transect of holes drilled along the Japan Trench margin, only single DSDP sites from select trench inner slope convergent margins had been drilled. Using this data (Lee et al., 1973; Bouma and Moore, 1975; Trabant et al., 1975; and Moore and Karig, 1976) and data from the Washington continental margin (Silver, 1972; Carson et al., 1974; Carson, 1977), a general model for convergent margin sediment geotechnical properties was developed. This model suggests that lower trench inner slope sediments are rapidly deformed and dewatered, resulting in highly overconsolidated sediments at shallow depths. The amount of deformation and the rate of change in geotechnical properties presumably decreases upslope away from the toe of the lower trench inner slope. Japan Trench margin drilling, however, recovered sediments with anomalous properties compared to those from previously drilled margins. Carson and Bruns (1980) report porosity values of

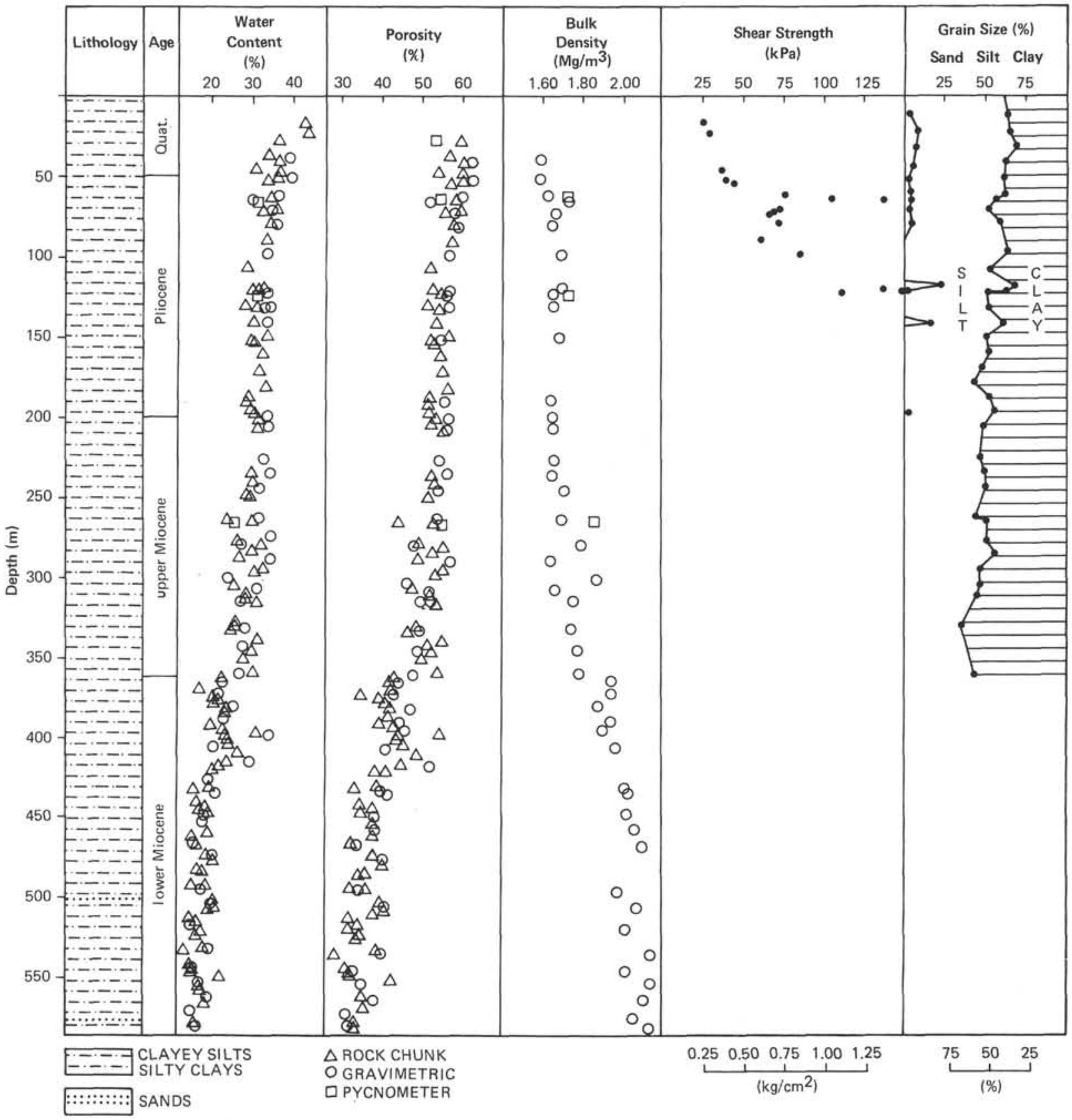

Figure 17. Geotechnical property summary profiles, Site 493.

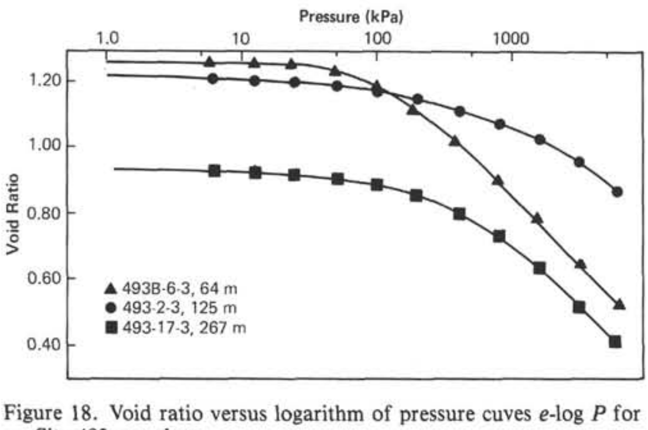

Figure 18. Void ratio versus logarithm of pressure cuves *e*-log *P* for Site 493 samples.

lower trench inner slope Site 441 sediments which exceed 60% at 550 meters sub-bottom. They indicate that the geotechnical property data from the Japan lower trench inner slope is representative of thick, overpressured, underconsolidated sediments. This interpretation agrees very well with Japan Trench Site 440 consolidation test results, which show underconsolidated sediments becoming increasingly more underconsolidated with depth (Shephard and Bryant, 1980).

Middle America Trench geotechnical properties appear somewhat anomalous also, in that values of porosity, bulk density, and water content are consistent with those determined from previously drilled convergent margin sites (Fig. 19), but the consolidation characteristics are much different. Lower trench inner slope

Table 6. Consolidation test results and geotechnical properties of samples tested from Site 493.

Core/Section	Depth below Seafloor (m)	Bulk Density (Mg/m^3)	Porosity (%)	Water Content (%)	Void Ratio	Effective Overburden Pressure (kPa)	Preconsolidation Pressure (kPa)	Overconsolidation Ratio
Hole 493B								
6-3	64	1.74	55.04	33.13	1.22	383	170	0.44
Hole 493								
2-3	125	1.74	53.52	31.15	1.15	983	250	0.26
17-3	267	1.87	46.56	25.32	0.87	1728	600	0.35

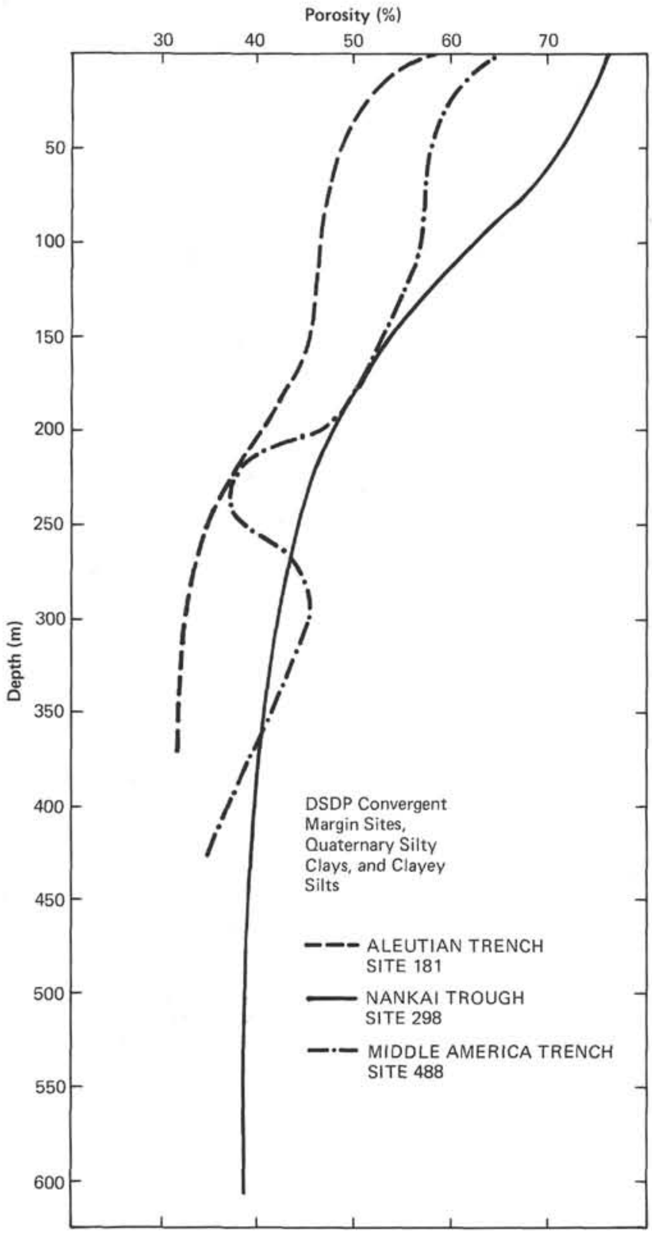

Figure 19. Porosity depth profiles for Quaternary clayey silt and silty clay sediments sampled in the Aleutian Trench, DSDP Site 181, Nankai Trough, DSDP Site 298, and Middle America Trench, DSDP Site 488.

Site 492 sediments above the zone of gas-related disturbance are overconsolidated, whereas Site 491 sediments become underconsolidated with depth. Site 488 sediments, located only 4 km landward of the trench axis near the toe of the lower inner slope, are underconsolidated.

Comparing *e*-log *P* curves from other convergent margin drill sites—DSDP Legs 31 (Sample 298-11-3, 297 m, Trabant et al., 1975) and 18 (Sample 181-28-1, 322 m; Lee et al., 1973)—and of surficial Sample 90-2 from the Washington continental slope (Carson, 1977) with Leg 66 results (Samples 488-30-1, 176 m, and 492-12-4, 108 m) illustrates the difference in consolidation characteristics (Fig. 20). An example of Japan Trench Site 440 *e*-log *P* curves is not shown because void ratios exceed 1.70 at depths greater than 550 meters. These data show that the break in slope used to compute the maximum presssure P_c to which a sediment has consolidated in the past occurs at a much lower pressure for Sample 488-30-1 than for any other sample. Overconsolidated sam-

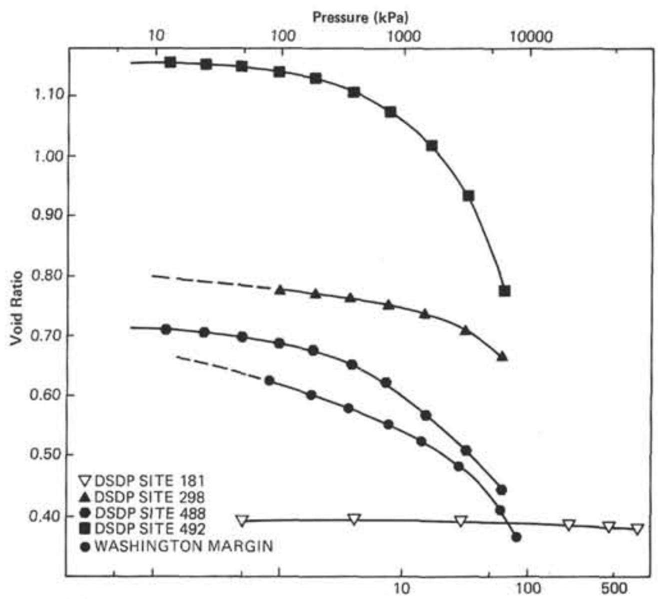

Figure 20. Consolidation test results, *e*-log *P* curves, of convergent margin sediments from DSDP Sites 181, 298, and 488 and from the Washington continental margin. Sample 90-2, showing the break in slope at low pressure (≃200 kPa) for Site 488, indicating underconsolidation. Curves from previously drilled convergent margin sites from Lee et al. (1973), Trabant et al. (1975), and Carson (1977).

ples from the Nankai Trough and particularly the Aleutian Trench show little change in void ratio under the maximum load applied in the laboratory. Although all samples except 90-2 from the Washington continental margin were obtained by standard DSDP rotary drilling and handling techniques, all are similar lithologically, and all were tested using one-dimensional consolidation apparatus, obvious differences in the state of consolidation are still apparent.

Samples 488-30-1 (265 m) and 488-33-6 (302.50 m) are located only 48 and 11 meters, respectively, above the first occurrence of thick sands. If these sands represent accreted trench sediments, the proximity of the two consolidation samples to these sands would suggest they are either accreted sediments or represent lower slope sediments which should have been directly affected by the accretion process. In either case the general geotechnical property model indicates these sediments should be overconsolidated and highly dewatered. However, if these sands were originally deposited on the lower trench inner slope and essentially deformed in place, the overlying clayey silt consolidation samples (488-30-1, 33–36 cm) would not represent sediments directly involved in the accretion process but represent deformed lower trench inner slope sediments instead. In this case one can only speculate on the consolidation state of deeper sediments which may represent accreted material.

Data utilized to develop the general geotechnical property model for active convergent margin sediments were obtained from margins having many similar site-specific parameters (Table 7). Trench sediment accumulation rates exceed 800 m/m.y. and result from a high clastic input. Convergence rates for these margins are low to moderate and range from approximately 2 cm/y. to 6 cm/y. (Atwater, 1970; Moore and Karig, 1976). This combination of high sediment accumulation rates and low convergence rates has resulted in a very thick trench sediment section. Horst and graben structures, normal faults or topographic irregularities on the oceanic plate as it descends into the subduction zone, are poorly developed or absent entirely. Seismic reflection profiles collected from these areas show uplifted anticlinal ridges, becoming progressively more faulted and folded landward along the lower trench inner slope (Hilde et al., 1969; Carson, 1977; Barnard, 1978). Combining these data with previously described geotechnical property results indicates that for "clastic-dominated" margins sediments are deformed by folding and faulting against the toe of the lower trench inner slope in the initial stage of the accretion process. Near-surface deforming sediments begin to dewater over relatively short drainage paths, becoming progressively overconsolidated through time.

Site-specific parameters for the Japan Trench margin (Table 7) include low sediment accumulation rates in the trench, high convergence rates (8 cm/y.–10 cm/y.), and a thin trench sediment section. Horst and graben structures are well developed on the oceanic plate, and deformation at the toe of the lower trench slope is not as pervasive as in the clastic-dominated margins. Geotechnical property data reveal high-porosity, low-density underconsolidated sediments which persist at depth. These data indicate that convergence at "pelagic-dominated" margins results in large quantities of high water content sediments descending below underconsolidated lower trench inner slope sediments. The pelagic sediments would be rapidly loaded and may dewater, causing abnormally pressured overlying sediments. Overpressured lower trench inner slope sediments would be deformed *in situ*.

Site-specific parameters of the Middle America Trench margin suggest it is intermediate between the clastic- and pelagic-dominated margins. Clastic sediment accumulation rates in the trench are substantial, but convergence rates of 7 cm/y. carry large volumes of pelagic sediments into the subduction complex. Deformation occurring along the lower trench slope is evident from geophysical, sedimentological, and geotechnical data. This deformation does not appear as pervasive as in clastic-dominated margins and has not resulted in highly overconsolidated sediments at shallow depths.

Table 7. Summary of general geotechnical property data and site-specific parameters for each of the margins discussed.

Convergent Margin	Middle America Trench DSDP Site 488	Aleutian Trench DSDP Site 181	Nankai Trough DSDP Site 298	Japan Trench DSDP Site 440	Washington Continental Margin
Oldest Age of Sediments Tested	Quaternary	Quaternary	Quaternary	Pliocene–late Miocene	Quaternary
Consolidation Characteristics	Underconsolidated	Highly Overconsolidated	Highly Overconsolidated	Underconsolidated	Highly Overconsolidated
Minimum Porosity (%)	33	32	35	55	36
Trench and Lower Slope Sedimentation Rate (m/m.y.)	$\simeq 350^b$	$\simeq 1700^a$	$\simeq 700^b$	$\simeq 200^b$	$\simeq 2000^a$
Trench Sediment Thickness (m)	$\simeq 600$	>1100	$\simeq 700$	$\simeq 500$	$\simeq 1300$
Convergence Rate (cm/y.)	$\simeq 7$	$\simeq 6$	$\simeq 2$	8–10	<2

Note: Data obtained from Molnar and Sykes, 1969; Atwater, 1970; Kulm et al., 1973; Lee et al., 1973; Trabant et al., 1975; Moore and Karig, 1976; Carson, 1977; Minster and Jordan, 1978; and von Huene, 1980.

[a] Trench.

[b] Lower slope.

Results of geotechnical investigations from both the Middle America Trench and the Japan Trench indicate that the convergence process does not always result in highly deformed low-porosity, overconsolidated sediments. Deformation in lower trench slope sediments may occur from the development of excess porewater pressures and oversteepened slopes related to the convergence process but not necessarily a direct result of accretion. Site-specific parameters should be carefully considered when analyzing the effects of the convergence process on sediment geotechnical properties.

ACKNOWLEDGMENTS

We greatly appreciate the assistance of DSDP and Global Marine personnel and are grateful to the shipboard scientific party for making Leg 66 an enjoyable venture. Special thanks and four "good core" awards are extended to W. Brennan, C. Deen, D. Marsee, and W. Meyers. T. C. Chamberlain and Hondo Crouch, imagineer, provided insight.

R. H. Bennett and W. E. Hottman reviewed the manuscript.

REFERENCES

Atwater, T., 1970. Implications of plate tectonics for the Cenozoic tectonic evolution of Western North America. *Geol. Soc. Am. Bull.*, 81:3513–3536.

Barnard, W. D., 1978. The Washington continental slope: Quaternary tectonics and sedimentation. *Mar. Geol.*, 27:79–114.

Bennett, R. H., Bryant, W. R., and Keller, G. H., 1977. Clay fabric and geotechnical properties of selected submarine sediment cores from the Mississippi Delta. *NOAA Prof. Pap.* 9, U.S. Department of Commerce.

Bennett, R. H., and Keller, G. H., 1973. Physical properties evaluation. *In* van Andel, Tj. H., Heath, G. R., et al., *Init. Repts. DSDP*, 16: Washington (U.S. Govt. Printing Office), 513–520.

Bouma, A. H., and Moore, J. C., 1975. Physical properties of deep-sea sediments from the Philippine Sea and Sea of Japan. *In* Karig, D. E., Ingle, J. C., Jr., et al., *Init. Repts. DSDP*, 31: Washington (U.S. Govt. Printing Office), 535–568.

Bowles, J. E., 1970. *Engineering Properties of Soils and Their Measurement:* New York (McGraw-Hill, Inc.).

Boyce, R. E., 1975. Definitions and laboratory techniques of compressional sound velocity parameters and wet water content, wet-bulk density, and porosity parameters by gravimetric and gamma ray attenuation techniques. *In* Schlanger, S. O., Jackson, E. D., et al., *Init. Repts. DSDP*, 33: Washington (U.S. Govt. Printing Office), 931–951.

———, 1977. Deep Sea Drilling Project procedures for shear strength measurement of clayey sediment using modified Wykeham Farrance laboratory vane apparatus. *In* Barker, P. F., Dalziel, I. W. D., et al., *Init. Repts. DSDP*, 36: Washington (U.S. Govt. Printing Office), 1059–1068.

Bredehoft, J. D., and Hanshaw, B. B., 1968. On the maintenance of anomalous fluid pressures: Thick sedimentary sequences. *Geol. Soc. Am. Bull.*, 81:1097–1106.

Carson, B., 1977. Tectonically induced deformation of deep-sea sediments off Washington and northern Oregon. *Mar. Geol.*, 24: 289–307.

Carson, B., and Bruns, T. R., 1980. Physical properties of sediments from the Japan Trench margin and outer trench slope: Results from DSDP Legs 56 and 57. *In* Scientific Party, *Init. Repts. DSDP*, 56, 57, Pt. 2: Washington (U.S. Govt. Printing Office), 1187–1200.

Carson, B., Yuan, J., Meyers, P. B., et al., 1974. Initial deep-sea sediment deformation at the base of the Washington continental slope: A response to subduction. *Geology*, 2:561–564.

Casagrande, A., 1936. The determination of the preconsolidation load and its practical significance. *Proc. Int. Conf. Soil Mech. Found. Eng. 3rd*, pp. 60–64.

Cernock, P. J., 1970. Sound velocities in Gulf of Mexico sediments as related to physical properties and simulated overburden pressures [Ph.D. dissert.]. Texas A&M University, College Station.

Demars, K. R., and Nacci, V. A., 1977. Significance of Deep Sea Drilling Project sediment physical property data. *Mar. Geotechnol.*, 3:151–170.

Hamilton, E. L., 1964. Consolidation characteristics and related properties of sediments from experimental Mohole (Guadalupe Site). *J. Geophys. Res.*, 69:4257–4269.

———, 1976. Variations of density and porosity in deep-sea sediments, *J. Sediment. Petrol.*, 46:280–300.

Hilde, T. W. C., Wageman, J. M., and Hammond, W. T., 1969. The structure of Tora Terrace and Nankai Trough off southwestern Japan. *Deep-Sea Res.*, 16:66–75.

Hottman, C. E., and Smith, J. H., 1978. Relationship among earth stresses, pore pressures and drilling problems offshore Gulf of Alaska, *Soc. Petr. Eng.*, 53rd Annual Tech. Conf., SPE7501, Houston.

Kulm, L. D., von Huene, R., et al., 1973. *Init. Repts. DSDP*, 18: Washington (U.S. Govt. Printing Office).

Lee, H. J., Olson, H. W., and von Huene, R., 1973. Physical properties of deformed sediments from Site 181. *In* Kulm, L. D., von Huene, R., et al., *Init. Repts. DSDP*, 18: Washington (U.S. Govt. Printing Office), 701–719.

Lowe, J., Zaccheo, P. F., and Feldman, H. S., 1964. Consolidation testing with back pressure. *Jour. Soil Mechanics and Foundation Division*, American Soc. Civil Engineers, 90:69–86.

Minster, J. B., and Jordan, T. H., 1978. Present day plate motions. *J. Geophys. Res.*, 80:5331–5354.

Mitchell, J. K., 1976. *Fundamentals of Soil Behavior:* New York (John Wiley & Sons).

Molnar, P., and Sykes, L. R., 1969. Tectonics of the Caribbean and Middle America regions from focal mechanisms and seismicity. *Geol. Soc. Am. Bull.*, 80:1639–1684.

Moore, J. C., and Karig, D. E., 1976. Sedimentology, structural geology, and tectonics of the Shikaku subduction zone, southwestern Japan. *Geol. Soc. Am. Bull.*, 87:1259–1268.

Nafe, J. E., and Drake, C. L., 1957. Physical properties of marine sediments. *In* Hill, M. N. (Ed.), *The Sea* (Vol. 3): New York (Interscience), 794–828.

Schmertmann, J. M., 1955. The undisturbed consolidation of clay. *Trans. Am. Soc. Civ. Eng.*, 120:1201–1233.

Seely, D. R., 1977. The significance of landward vergence and oblique structural trends on trench inner slopes. *Island arcs, Deep Sea Trenches and Back-arc Basins: American Geophysical Union Maurice Ewing Series* 1, pp. 187–198.

Shephard, L. E., and Bryant, W. R., 1980. Consolidation characteristics of Japan Trench sediments. *In* Scientific Party, *Init. Repts. DSDP*, 56, 57, Pt. 2: Washington (U.S. Govt. Printing Office), 1201–1206.

Silva, A. J., 1975. Marine geomechanics—an overview and projections. *Deep-sea Sediments—Physical and Mechanical Properties:* New York (Plenum Press), pp. 45–76.

Silver, E. A., 1972. Pleistocene tectonic accretion of the continental slope off Washington. *Mar. Geol.*, 13:239–250.

Skempton, A. W., 1970. The consolidation of clays by gravitational compaction. *Q. J. Geol. Soc. London*, 125:373–411.

Trabant, P. K., Bryant, W. R., and Bouma, A. H., 1975. Consolidation characteristics of sediments from Leg 31 of the Deep Sea Drilling Project. *In* Karig, D. E., Ingle, J. C., Jr., et al., *Init. Repts. DSDP*, 31: Washington (U.S. Govt. Printing Office), 569–572.

von Huene, R., Aubouin, J., Azema, J., et al., 1980. Leg 67: The Deep Sea Drilling Project Mid-America Trench off Guatemala. *Geol. Soc. Am. Bull.*, 91:421–432.

Woodbury, H. O., Spotts, J. H., and Ahres, W. H., 1978. Gulf of Mexico continental slope sediments and sedimentation. *In* Bouma, A. H., Moore, G. T., and Coleman, J. M. (Eds.), *Framework, Facies and Oil Trapping Characteristics of the Upper Continental Margin.* AAPG Studies in Geology, Tulsa: (American Association of Petroleum Geologists), pp. 117–138.

APPENDIX
Leg 66 Geotechnical Property Measurements

				Continuous GRAPE		Two-Minute GRAPE			Rock Chunk or Gravimetric[a]			Air Pycnometer				Velocity (km/s)	
Core	Section	Interval (cm)	Sub-bottom Depth (m)	Bulk Density (Mg/m³)	Porosity (%)	Bulk Density (Mg/m³) Parallel	Bulk Density (Mg/m³) Normal	Porosity (%)	Water Content (%)	Porosity (%)	Bulk Density (Mg/m³)	Water Content (%)	Porosity (%)	Bulk Density (Mg/m³)	Shear Strength (kPa)	Parallel	Normal
Hole 487																	
2	1	109-112	2.1						51.77	74.60					4.93		
2	2	109-112	3.6						52.12	74.80					3.28		
2	3	109-112	4.7						53.10	75.54							
2	4	109-112	5.8	1.385	78.49				52.42	75.02					2.67		
3	1	86-88	11.38									135.8	78.24	1.40			
3	1	89-92	11.40						57.32	78.56					4.72		
3	2	29-31	12.45	1.408	77.15				57.32[a]	78.45	1.37						
3	2	44-47	12.60						59.08	79.76							
3	3	59-62	14.10						57.94	78.95							
3	4	59-62	15.60	1.418	76.52				55.56	77.32							
3	5	29-31	16.80	1.408	77.15				54.47[a]	76.62	1.41						
3	5	89-92	17.40						55.96	77.62					3.80		
5	1	129-131	30.80						56.82[a]	78.56	1.38				13.54		
5	2	18-20	31.20									154.0	79.87	1.38			
5	2	109-112	32.10	1.400	77.60				54.09	76.28					11.18	1.452	
5	3	130-132	33.81	1.409	77.09				52.59[a]	75.29	1.43				8.62	1.408	
6	1	109-112	40.10						54.09[a]	78.02	1.479				16.31		
6	2	19-21	40.70	1.440	75.20				57.51	78.68					24.01		
6	3	29-31	42.30	1.440	75.20				57.22	78.47					10.06	1.474	
6	3	109-112	43.10	1.414	76.77				54.27	76.41					14.70	1.442	
7	1	119-122	49.70						57.49	78.65					11.08		
8	1	84-87	58.85						56.08	77.71					10.26		
8	3	19-22	61.20						57.24	78.49					14.95		
8	3	109-111	62.10						56.99[a]	78.57	1.38				35.09		
8	4	19-21	62.70	1.410	77.03				59.00[a]	79.95	1.36				31.28		
8	4	118-120	63.70									142.0	79.69	1.39			
8	5	9-11	64.10						55.60[a]	77.74	1.40				14.66		
8	5	109-112	65.10						57.05	78.41					17.24	1.441	
8	6	59-61	66.10	1.414	76.77				56.46[a]	78.16	1.38				19.55	1.472	
9	1	99-102	68.50						57.60	78.77					19.90		
9	3	19-22	70.70						54.11	76.28					10.26		
9	3	119-121	71.70						56.23[a]	78.18	1.39				14.98		
9	4	39-41	72.40	1.391	78.17				56.15[a]	78.05	1.39				43.60		
9	5	50-52										141.0	78.56	1.41			
9	6	58-61	75.60	1.408	77.15				56.02	77.90					15.93		
10	1	99-102	78.00						52.38	75.08					16.01		
10	2	29-32	78.80	1.418	76.52				53.20	75.64					11.24		
10	4	131-133	82.82	1.410	77.03				54.33[a]	76.66	1.410				48.43		
10	5	19-22	83.20						52.87	75.39					43.00		
10	5	115-117	84.15									115.7	75.52	1.45			
10	6	84-86	85.35	1.470	73.46				49.66[a]	72.64	1.47				38.78	1.487	
11	1	117-120	87.68						53.39	75.77					13.75		
11	2	120-122	89.20									123.9	77.27	1.42			
11	3	95-98	90.46						53.30	75.65					12.11		
11	4	79-81	91.80	1.392	78.11				58.63[a]	79.65	1.36				39.19	1.493	
12	3	8-11	99.10						65.37	85.19						1.478	
12	3	119-121	100.20	1.232	87.65				63.87[a]	81.94	1.28				38.10		
12	4	78-81	101.30						62.85	83.77					70.68		
12	5	47-49	102.48						67.64[a]	83.74	1.24				43.00	1.535	
13	3	98-101	109.5						63.35	84.04					92.77		
13	4	18-21	110.2	1.389	78.30				63.56	84.24					38.29		
13	4	123-126	111.25						56.31	79.68					38.29		
13	4	79-81	110.8						55.00[a]	76.98	1.40					1.535	
13	5	14-16	111.65						53.05[a]	75.83	1.43				107.49	1.490	
14	1	108-111	116.10	1.377	79.00				59.25	81.60					82.46		
14	2	89-92	117.38						55.66[a]	77.61	1.39				66.26	1.452	
14	3	50-52	118.50									179.0	84.42	1.34			
14	3	113-116	119.15	1.472	73.33				60.20	82.16						1.471	
15	2	128-131	127.80	1.317	82.57				69.30	87.30					42.70		
15	3	113-116	128.55						71.15	88.25					50.80	1.490	
15	4	109-111	130.10	1.302	83.45				70.49[a]	86.99	1.23				46.38		
15	5	88-91	131.40						69.66	87.48					81.72	1.461	
15	6	108-110	133.09	1.249	86.64				74.03[a]	88.61	1.20				77.31		
16	1	34-36	134.34						65.70[a]	84.02	1.28					1.483	
16	2	84-86	136.35	1.260	86.00				71.51[a]	86.58	1.21					1.454	
18	2	99-101	155.50	1.404	77.34				58.00[a]	80.13	1.38				85.41		
18	4	128-131	158.80	1.431	75.75				58.16	80.90					78.19		
18	5	100-103	160.00									215.9	87.11	1.29			
Hole 488																	
2	1	100-103	2.0						46.62	69.89					4.31		
2	2	20-23	2.70												6.36		
2	2	90-93	3.40						43.80	67.50					8.21		
2	3	50-52	4.50									84.4	68.84	1.53			
2	3	110-113	5.10						45.45	68.91					7.39		
2	4	99-102	6.50						43.96	67.59					10.88		
3	1	129-132	11.80														
3	1	140-143	11.9						42.15[a]	64.47	1.53				9.64		
3	1	49-52	11.0						42.5	66.28					7.18		
3	2	128-140	13.30	1.41	77.03												
3	2	9-12	12.10						41.70	65.54					8.21		
3	2	50-52	12.50									71.4	65.36	1.59			
3	2	119-122	13.20						40.1	64.03					7.39		
4	1	99-103	21.0						31.81	55.37					10.87		
4	2	137-140	22.9						37.03	60.98					14.77		
4	3	27-30	24.25						38.95	62.92					14.56		
4	3	126-129	23.30						38.16[a]	61.18	1.60				16.61		
4	4	63-66	25.13						35.50[a]	58.15	1.64				19.69		
4	5	99-102	27.00						40.47	64.38					21.74		
4	5	138-150															
4	6	54-57	28.05						40.76	64.65					19.28		

				Continuous GRAPE		Two-Minute GRAPE			Rock Chunk or Gravimetric[a]			Air Pycnometer				Velocity (km/s)	
						Bulk Density (Mg/m^3)											
Core	Section	Interval (cm)	Sub-bottom Depth (m)	Bulk Density (Mg/m^3)	Porosity (%)	Parallel	Normal	Porosity (%)	Water Content (%)	Porosity (%)	Bulk Density (Mg/m^3)	Water Content (%)	Porosity (%)	Bulk Density (Mg/m^3)	Shear Strength (kPa)	Parallel	Normal
Hole 488 (Cont.)																	
4	6	100–102	29.00									50.8	57.20	1.73			
5	2	28–30	31.30						40.48	64.40							
5	2	43–46	31.45						40.73	64.62					24.61		
5	3	88–91	33.4						39.65[a]	61.73	1.56				13.95		
5	6	67–70	37.7						37.43[a]	59.97	1.60				21.33		
5	6	138–141	38.4						36.24	60.19							
9	1	48–51	68.00						32.30	55.91					41.76		
9	1	141–143	68.91						33.51[a]	56.18	1.68				27.70		
9	2	23–26	69.25						35.05	58.99					47.19		
9	2	127–130	70.3						37.49[a]	60.40	1.61				47.36		
9	3	100–103	71.5						36.10[a]	59.01	1.63				28.11		
10	1	50–52	77.50									52.5	56.28	1.71			
10	1	119–122	78.2						34.89	58.76					12.52		
10	2	102–105	79.55						37.37[a]	59.49	1.59						
10	3	129–131	81.30						33.97	57.77					19.14		
10	4	64–67	82.15						34.35[a]	57.28	1.67				17.67		
11	1	90–93	87.40									53.4	59.31	1.68			
11	1	93–96	87.45												16.93		
11	2	127–130	89.30						33.62	56.83	1.69				51.54		
11	5	127–130	93.80						32.82	56.50					53.01		
11	6	48–51	94.50						34.96[a]	57.49	1.64				49.84		
13	1	17–20	105.70						32.62[a]	55.61	1.70				43.98		
13	2	0–02	107.00						34.93	58.80					34.21		
13	3	40–42	108.9						36.97[a]	59.12	1.60				38.12		
13	4	40–42	110.40									58.1	59.63	1.67			
14	1	113–116	116.15						34.86	58.73					63.32		
14	1	140–142	116.40									50.5	57.15	1.72			
15	1	58–61	125.10						32.71	56.38					46.91		
15	1	135–137	125.85						38.28[a]	59.86	1.56				29.32		
16	1	123–125	135.25						34.31[a]	58.80	1.62				46.91		
16	1	125–128	135.28									44.30	51.31	1.80			
16	2	103–106	136.55						30.95	54.38					50.82		
16	4	50–53	139.00						32.55[a]	54.68	1.68						
18	1	40–43	153.40						27.06[a]	48.56	1.79				47.89		
18	3	18–21	156.20						32.98	56.68					84.67		
18	5	115–118	160.15						27.69[a]	49.59	1.79				86.14		
18	5	135–137	160.35									34.9	48.09	1.88			
19	1	38–41	162.9						27.42	50.11					87.96		
19	1	45–48	162.95									37.9	49.97	1.84			
19	3	7–10	165.6						28.44[a]	49.69	1.75				85.52		
19	4	8–11	167.1						29.98[a]	51.42	1.71				86.01		
20	1	98–100	173.00									44.5	52.52	1.79			
20	1	111–114	173.12	1.605	65.38				30.67[a]	52.32	1.71				78.19		
20	2	98–101	174.5						30.33	53.65					85.5		
20	3	16–19	175.16												85.5		
21	1	135–138	182.85									55.50	55.55	1.727	105.07		
21	2	08–10	183.10									40.00	49.42	1.84			
21	2	28–30	183.3						29.58	52.76					102.62		
21	2	133–136	184.35			1.79		54.15	27.98[a]	49.59	1.77				90.41		
21	5	95–98	188.45						28.14[a]	49.66	1.76				78.19		
21	6	9–12	189.10												87.96		
22	2	19–22	192.70						28.56[a]	50.53	1.77				87.96		
22	2	119–122	193.70						25.51	47.66					83.08		
22	3	18–20	194.20									39.20	49.24	1.87			
22	3	119–122	195.20						28.41	51.34					146.6		
23	1	58–61	201.10						28.97[a]	50.80	1.75				97.76		
24	1	78–81	210.80						18.12[a]	36.34	2.01						
24	1	85–87	210.85									22.59	35.78	2.08			
24	1	118–121	211.2	1.925	46.29				22.14[a]	42.93	1.934						
25	1	112–115	220.65	1.875	49.28				21.69[a]	42.37	1.95						
26	2	118–121	231.7	1.917	46.73				15.95	33.54					61.08		
26	2	135–138	231.85									21.91	35.89	2.08			
26	3	83–86	232.85	1.943	45.20	2.022		40.45	16.45	34.36							
26	3	86–88										21.20	34.61	2.12			
26	4	94–97	234.45	1.943	45.20				17.87[a]	36.61	2.05						
26	5	63–66	235.65	2.066	37.82				14.18	30.52							
26	5	122–125	236.25						15.74	33.19							
26	6	75–78	237.25						17.41	35.49							
26	6	135–138	237.85						14.55	31.17							
27	1	118–120	239.7	1.953	44.57				19.04[a]	38.68	2.03						
29	2	130–132	260.3									22.00	37.29	2.09			
29	3	9–12	260.6	1.975	43.30												
29	4	71–74	262.72	1.975	43.30				19.83	39.68							
29	5	8–11	263.6						20.71[a]	40.96	1.98						
29	CC	6–9	265.06						26.43[a]	49.22	1.86						
29	CC	9–12	265.10									24.70	39.17	2.034			
30	1	93–96	265.45						23.34	44.73							
30	1	145–147	265.95									27.40	40.95	1.99			
30	2	93–96	266.95						20.47	40.63							
30	3	81–83	268.32	1.932	45.84				20.28	40.11	1.98						
30	3	93–96	268.45						18.65	37.87							
30	3	129–131	268.75						17.69[a]	36.40	2.06						
30	4	18–20	269.15									31.3	43.35	1.96			
30	4	93–96	269.95						23.54	45.01							
30	5	86–96	271.40	1.907	47.37				22.33	43.33							
30	6	91–94	272.92	1.932	45.84				20.99	41.40							
31	1	53–56	276.55			2.048		38.95	22.33	43.33							
31	2	53–56	278.05			1.901		47.70	22.86	44.07							
31	3	53–56	279.55	1.914	46.92	1.956		44.41	23.29	44.67							
31	3	61–64	279.62						24.02[a]	45.6	1.90						
31	CC	00–02	284.50									34.30	49.19	1.93			

				Continuous GRAPE		Two-Minute GRAPE			Rock Chunk or Gravimetric[a]			Air Pycnometer				Velocity (km/s)	
Core	Section	Interval (cm)	Sub-bottom Depth (m)	Bulk Density (Mg/m^3)	Porosity (%)	Bulk Density (Mg/m^3) Parallel	Bulk Density (Mg/m^3) Normal	Porosity (%)	Water Content (%)	Porosity (%)	Bulk Density (Mg/m^3)	Water Content (%)	Porosity (%)	Bulk Density (Mg/m^3)	Shear Strength (kPa)	Parallel	Normal
Hole 488 (Cont.)																	
32	1	87–90	285.90			1.910		47.18	21.50	42.14							
32	2	80–83	287.32			2.155		32.55	21.01	41.43							
32	3	75–78	288.76			2.170		31.64	20.54	40.74							
32	4	75–78	290.26			2.015		40.88	22.44	43.48							
32	5	8–11	291.10						22.96[a]	44.4	1.93						
32	4	43–45	289.96						22.64[a]	44.27	1.96						
33	1	52–55	294.54			2.23		28.14	24.56	46.40							
33	1	103–106	296.55			2.01		41.49	23.87	45.47							
33	2	132–135	296.85						25.64	47.83							
33	3	61–64	297.62			2.07		37.61	23.28	44.66							
33	4	118–121	299.7			2.04		39.16	21.11	41.57							
33	5	65–68	300.65			1.998		41.91	22.37	43.38							
33	6	50–55	302.00									28.2	38.01	2.123			
33	6	95–98	302.45						24.29[a]	45.56	1.88						
34	1	95–98	303.96			2.058		38.36	19.02	38.44							
34	2	74–77	305.25						21.19[a]	45.54	1.88						
34	3	78–81	306.80						23.77[a]	44.64	1.87						
34	4	128–131	308.80			1.910		47.19	21.70	42.43							
34	4	128–131	308.80						23.65	44.36	1.88						
39	1	78–82	353.3			2.08		37.25	15.60	32.95							
40	1	78–82	362.8						19.15[a]	37.93	1.98						
40	1	137–139	363.39			2.15		32.59	11.13	24.98							
40	1	146–148	363.47			2.16		32.42	18.35	37.41							
42	1	141–144	382.43			2.02		40.69	21.05	41.49							
42	2	13–16	382.65			2.05		38.60	18.52	37.67							
42	2	27–30	382.80			2.12		34.47	19.25	38.80							
42	3	26–29	384.26	1.92	46.41												
42	3	30–32	384.28									29.17	42.51	1.954			
43	1	140–143	391.9			2.27		25.64	19.37	38.98							
44	1	23–25	400.23			1.945		45.08	15.26	32.38							
46	1	105–107	420.05									19.50	34.12	2.12			
Hole 489A																	
1	1	140–143	1.40						34.17	58.49							
1	2	8–10	1.60	1.84	51.59											1.679	
1	2	124–128	2.75						30.12	53.91					25.65		
1	3	13–16	3.15						35.54[a]	60.30	1.70						
1	3	78–81	3.80						28.94	52.50					11.70		
1	4	80–83	5.30	1.93	45.83	2.03		39.74							11.49	1.697	
2	1	123–128	7.25						29.79	53.52					50.89		
2	2	130–133	8.80						28.28	51.70					37.14		
2	3	76–79	9.75						30.05	54.36					118.54		
2	4	13–15	10.65									30.12	52.93	1.82			
2	4	59–62	11.10	1.85	50.57				29.21[a]	52.83	1.80					1.599	
2	4	106–109	11.55												86.88		
2	5	14–17	12.15														
2	5	117–120	13.15			1.92		46.75	29.04	52.62					67.37		
2	6	25–28	13.75	1.83	52.11				32.81[a]		1.83				62.58		
2	6	114–118	14.68						32.36						67.74		
3	5	143–145	22.95	1.84	51.25	1.99		41.82	29.86	53.61					173.76	1.607	
4	1	147–150	26.50			2.08		36.76	26.67	49.68							
4	2	143–147	27.95			2.01		41.15	25.00	47.50							
4	1	27–30	55.30			2.04		39.43	19.89	40.26							
4	1	103–107	56.05			2.09		36.02	22.71[a]	44.42	1.96						
4	2	93–96	57.45	2.04	39.24				17.74	36.92							
4	3	63–67	58.65						21.05[a]	42.00	1.99						
4	4	135–138	59.35									19.16	39.58	2.048			
4	4	16–20	59.70	1.98	43.22				20.74	41.53						1.658	
4	5	98–100	62.00			2.00		41.79	20.54	41.23							
4	CC	7–10	64.60						19.53	39.71						1.541	
5	1	18–22	65.20						19.29	39.35							
5	2	19–22	66.70	1.98	43.20												
5	4	101–104	70.53	1.90	47.58				28.04[a]	52.54	1.84						
6	1	147–150	76.00						25.96	48.76							
6	2	58–61	76.60	1.78	54.90				20.53	41.22							
6	3	40–43	77.90	1.89	48.64	1.90		47.91	30.53[a]	54.18	1.77						
7	1	60–65	84.65			2.08		37.25	22.34[a]	43.86	1.96						
7	2	71–75	86.25	1.92	46.77	2.01		41.32	22.25	43.72						1.502	
7	3	98–102	88.00						18.32	37.84						1.475	
7	5	18–20	90.20									22.72	45.14	1.99			
8	1	49–53	94.00			1.95		45.09	23.32	45.22							
8	2	49–51	95.50						28.88[a]	52.49	1.82						
8	3	12–15	96.65	1.83	51.88	1.90		47.68	26.63[a]	49.57	1.86					1.763	
9	2	147–150	106.00			1.86		49.93	28.08	51.45							
9	3	3–5	106.05									27.64	49.96	1.88			
9	3	5–7	106.05													1.813	
10	1	3–7	112.55			2.02		40.64	22.72	44.38						1.633	
10	CC	3–7				1.92		46.93	21.57[a]	42.53	1.97						
11	1	146–150	123.50			2.02		40.68	22.82	44.52							
11	2	89–93	124.40			1.94		45.32	34.90	47.36						1.924	
11	3	110–113	126.10	1.83	52.16				21.57[a]	42.53	1.97						
12	1	119–121	132.70			2.09		37.06	21.70[a]	42.63	1.96						
12	2	133–136	134.35													4.248	
13	2	10–12	142.60									23.25	44.09	1.97			
13	2	10–12	142.60			2.02		40.49									
13	3	88–90	143.40	1.86	49.98	2.08		36.83	19.83[a]	40.18	2.03					1.978	
15	1	13–16	160.15			1.98		42.57	22.63[a]	43.72	1.93					1.707	
16	2	52–54	166.53			1.99		42.34	21.65[a]	42.82	1.98					1.841	
16	3	130–133	168.62	1.84	51.51	2.03		40.27	21.10[a]	42.13	1.98					1.779	
16	4	23–25	169.25									23.25	43.98	1.95			
16	4	23–27	169.25						23.54	45.52							

Core	Section	Interval (cm)	Sub-bottom Depth (m)	Continuous GRAPE Bulk Density (Mg/m^3)	Continuous GRAPE Porosity (%)	Two-Minute GRAPE Bulk Density (Mg/m^3) Parallel	Two-Minute GRAPE Bulk Density (Mg/m^3) Normal	Two-Minute GRAPE Porosity (%)	Rock Chunk or Gravimetric[a] Water Content (%)	Rock Chunk or Gravimetric[a] Porosity (%)	Rock Chunk or Gravimetric[a] Bulk Density (Mg/m^3)	Air Pycnometer Water Content (%)	Air Pycnometer Porosity (%)	Air Pycnometer Bulk Density (Mg/m^3)	Shear Strength (kPa)	Velocity (km/s) Parallel	Velocity (km/s) Normal
Hole 489A (Cont.)																	
17	1	98–101	170.5			2.05		38.63	22.78	44.46						1.816	
17	2	43–45	171.45									25.48	46.85	1.92			
17	2	45–47	171.45	1.81	53.02	1.99		42.65	23.70[a]	45.24	1.91						
18	1	98–101	180.00						24.07								
18	2	99–102	181.50	1.84	51.25				22.09[a]	44.22	2.00						
18	3	103–106	183.05						18.98[a]	36.97	2.05						1.880
19	1	8–10	183.10	1.81	53.26				21.02	41.94							1.695
19	3	91–93	186.92			2.18		31.10	17.55	36.62							1.796
19	CC	7–10				2.14		33.38									1.763
19	1	90–92	183.90			2.10		35.95	17.28[a]	35.89	2.08						
20	CC	8–11				2.09		36.54	19.78[a]	39.24	1.98						
21	3	118–122	202.20			2.17		31.34	20.93	41.84							
21	4	28–31	202.80			2.15		32.83	20.12	40.60							
21	5	49–52	204.50	1.82	49.65	2.16		32.10	17.59[a]	36.28	2.06						
21	6	24–27	205.75			2.16		32.10	19.75	40.05							
22	2	101–104	210.03						16.91[a]	35.22	2.08						
22	3	103–107	211.05						17.14	35.96							
22	4	58–61	212.60						16.13	34.30							
22	5	93–96	214.46						17.36	36.31							
23	2	128–132	219.80	1.85	50.82				2.04							4.677	
23	4	47–51	222.00						15.06	32.49							
24	2	102–106	229.05			2.19		30.14	16.77	35.35							
24	3	39–43	229.90	1.85	50.82				16.77	35.35							
24	4	13–15	231.15									15.12	31.32	2.18			
24	4	28–32	231.30						15.23[a]	32.42	2.13						1.684
24	6	74–78	234.75														
25	1	37–42	236.40	1.85	50.53				15.74	35.30							
25	4	46–50	241.0						17.59	36.68							
25	4	134–138	241.75						14.98[a]	32.02	2.14						1.899
25	6	23–27	243.75						16.15	34.33							
26	2	65–70	247.70	2.09	36.22				14.90[a]	32.24	2.16						
26	4	87–91	250.90	2.15	32.98				11.59[a]	26.05	2.25						
27	2	26–31	256.80	1.86	50.02				17.57	36.65							
27	3	55–60	258.60	2.08					17.48[a]	36.70							
28	3	53–57	267.55						13.18	29.18							1.675
28	4	0–5	268.55						14.23[a]	30.50	2.14						
29	2	0–3	274.53														
29	3	0–3	276.03														
29	5	2–5	279.05	1.90	47.84												
30	5	2–5	288.05						14.08[a]	30.46	2.16						
30	5	106–110	289.10														3.984
30	5	63–66	288.65						13.52	29.79							
31	2	91–94	293.43						13.98	30.61							
Hole 490																	
1	1	127–131	1.27						43.3	66.84					20.21		
1	2	57–60	2.10						44.6[a]	68.40	1.53						
1	2	142–147	2.95						34.2	57.84					11.70		
1	3	45–48	3.45														
1	3	130–134	4.30						47.6	70.57					28.73		
1	4	08–12	4.60						42.7[a]	66.4	1.56				36.11	1.558	
1	4	108–112	5.60												32.11		
1	CC	04–08							37.1	60.89					30.16		
2	1	58–62	9.60						43.9	67.83					34.20		
2	1	143–145	10.45						43.7	67.2					26.06		
2	2	122–126	11.75						40.9	64.6					21.98		
2	3	133–137	13.35						42.3	65.9	21.49						
2	4	96–100	14.50						38.2[a]	61.8	1.62				56.84	1.538	
2	5	116–120	16.20						36.4	60.2					44.94		
2	6	98–103	17.50						40.5	64.2					56.94		
3	2	137–141	21.40						37.7	61.5					47.85		
3	3	101–103	22.51						33.4	57.0					57.43		
3	4	102–106	24.05						34.1[a]	57.0	1.67				47.86		
3	5	106–109	25.59						35.4	59.13					34.60		
3	6	81–84	26.82						36.3	60.07					36.08		
3	7	117–121	28.70												40.49		
4	2	108–112	30.6						35.2	58.92					72.89		
4	3	139–142	32.40						37.9[a]	61.4	1.62				80.99		
4	4	50–53	33.00						34.6	58.28					59.32		
4	5	61–65	34.65						34.4	58.06					44.18		
5	6	102–105	46.55						32.2	55.63					55.96		
5	CC	7–10	47.10						36.3[a]	58.5	1.61				45.92		
5	CC	18–20	47.20									56.9	58.88	1.701			
6	5	140–143	54.40						38.4[a]	60.9	1.59				112.64		
6	5	63–67	53.65						37.1	60.89							
7	1	76–80	57.30						33.0	56.53					59.64		
7	2	66–70	58.7			1.85		50.93	40.7[a]	63.7	1.56						
7	3	123–127	60.75						39.6[a]	62.5	1.58				122.22		
7	3	51–53	60.02									65.7	62.05	1.63			
8	1	116–120	67.20						35.4	59.13							
8	2	102–106	68.55						36.4[a]	59.4	1.63				71.42		
8	3	121–125	70.25						34.5	58.17					106.76		
8	4	101–104	71.53			1.99		42.64	40.0[a]	62.6	1.57				105.28		
9	1	121–125	76.75						34.7[a]	57.2	1.65				88.35		
9	2	30–34	77.30												77.31		
9	2	135–138	78.35						35.8	59.55					87.93		
9	5	48–51	82.00			1.95		44.90									
10	1	70–74	86.24						37.4	61.20					100.15		
10	1	137–141	86.90						38.0	61.80					75.83		
10	2	139–143	88.40						36.8[a]	59.4	1.61				73.28		
10	3	33–37	88.85						34.7	58.38					90.37		

				Continuous GRAPE		Two-Minute GRAPE			Rock Chunk or Gravimetric[a]			Air Pycnometer				Velocity (km/s)	
Core	Section	Interval (cm)	Sub-bottom Depth (m)	Bulk Density (Mg/m^3)	Porosity (%)	Bulk Density (Mg/m^3) Parallel	Bulk Density (Mg/m^3) Normal	Porosity (%)	Water Content (%)	Porosity (%)	Bulk Density (Mg/m^3)	Water Content (%)	Porosity (%)	Bulk Density (Mg/m^3)	Shear Strength (kPa)	Parallel	Normal
Hole 490 (Cont.)																	
10	4	58–61	90.60						33.9	57.52					109.91		
11	1	49–51	95.01						36.0	59.76	1.60				87.9		
12	2	52–56	106.05						33.4	56.97							
12	2	93–96	106.45						34.3[a]	56.8	1.66				109.9		
12	2	134–137	106.85														
15	1	120–124	133.70						30.1	53.20							
15	2	138–141	135.40														
15	3	64–67	136.15						31.0	54.26							
15	4	21–26	137.25						30.7	53.91							
15	5	54–59	139.05														
15	6	30–35	140.25														
16	1	98–101	143.0						32.3	55.74							
16	2	63–67	144.15						31.5	54.83							
16	3	29–33	145.30						34.1[a]	55.8	1.64						
16	3	40–43	145.40						33.7[a]	58.1	1.72						
16	3	76–79	145.78														
16	3	76–79	145.78														
16	4	5–7	146.55														
17	1	105–108	152.55						33.8	57.41							
17	2	119–123	154.20						32.3	55.74							
17	3	57–61	155.10						30.8	54.02							
17	4	49–53	156.50			1.765		55.81	31.0[a]	53.1	1.71						
17	4	49–53	156.50						29.7	52.73							
17	4	73–75	156.25									46.6	54.20	1.742			
18	1	63–66	161.65						33.3	56.86							
18	2	114–117	163.65						33.0	56.53							
18	3	33–36	164.35						31.5	54.83							
18	4	56–59	166.58						27.8	50.41							
18	4	120–123	166.73						27.20	49.66							
18	4	123–125	166.76														
18	5	10–12	167.10														
18	5	31–33	167.32						28.8	51.64							
19	1	143–146	171.95						28.6	51.40							
19	2	53–56	172.55														
20	1	103–107	181.05						30.7	53.91							
20	2	91–94	182.43						31.0	54.26							
20	2	127–131	182.78						32.6[a]	55.5	1.70						
20	3	27–32	183.30									38.6	50.28	1.83			
20	3	129–132	184.30						27.7	50.29							
20	4	93–94	185.44						30.7[a]	52.5	1.71						
20	4	94–97	185.45						30.0	53.08							
20	5	76–80	186.80														
20	6	77–81	188.30						32.2	55.63							
21	1	126–131	190.80						33.6	57.19							
21	2	135–139	192.35						82.9	56.42							
21	3	110–112	193.60						30.7	53.91							
21	4	53–57	194.55						30.5[a]	53.1	1.74						
21	4	76–79	194.76						31.4	54.72							
21	5	92–96	196.45						29.8	52.85							
21	6	86–90	197.90						29.3[a]	51.7	1.76						
22	1	129–133	200.30						27.7	50.29							
22	2	119–123	201.70						27.4	49.91							
22	3	91–94	202.92						31.2	54.49							
22	4	80–83	204.30						28.6[a]	50.8	1.78						
22	5	85–89	205.85						29.22	52.15							
22	6	20–27	207.25						28.1[a]	49.5	1.76						
23	1	130–132	209.80						31.1	54.37							
23	2	45–48	210.45						30.6	53.79							
23	3	74–77	212.25						33.0	56.53							
23	4	40–44	213.40						32.0[a]	55.0	1.72						
23	5	55–58	215.05						31.5	54.83							
23	6	49–53	216.50						28.6[a]	51.4	1.80						
23	6	102–105	217.55						26.9	49.28							
23	7	67–71	218.10						23.7	45.06							
24	1	118–120	218.2						26.1	48.25							
24	2	93–97	220.4						25.9[a]	48.1	1.86						
24	3	110–114	222.10						24.1	45.60							
24	4	94–97	223.45														
25	1	27–31	227.80						27.4	49.91							
25	2	121–124	230.72						30.2[a]	52.9	1.75						
25	3	46–49	230.98						27.8	50.41							
25	4	91–94	232.92						28.1[a]	51.0	1.81						
25	5	13–17	233.65						26.0	48.12							
25	6	131–133	236.32														
26	3	06–08	240.06						26.32	48.54							
26	4	52–57	242.05						28.9[a]	52.0	1.80						
26	5	100–105	244.00						24.7	46.41							
26	6	101–105	245.55														
27	1	105–108	247.55						21.4	41.82							
27	2	118–122	249.20						21.2	41.53							
27	3	82–86	250.35														
28	1	86–89	256.86						24.9	46.68							
28	2	76–79	258.26						27.6	50.16							
28	3	78–82	259.80						27.7	50.29							
28	3	119–122	260.20						28.5[a]	51.0	1.79						
28	4	73–77	261.25						26.7	49.02							
28	5	73–76	262.76						27.0	49.40							
28	5	109–112	263.11						25.2[a]	47.7	1.89						
28	6	80–83	264.30						25.0	46.80							
29	1	131–134	266.83						29.00	51.88							
29	2	120–124	268.2														

				Continuous GRAPE		Two-Minute GRAPE			Rock Chunk or Gravimetric[a]			Air Pycnometer				Velocity (km/s)	
Core	Section	Interval (cm)	Sub-bottom Depth (m)	Bulk Density (Mg/m³)	Porosity (%)	Bulk Density (Mg/m³) Parallel	Bulk Density (Mg/m³) Normal	Porosity (%)	Water Content (%)	Porosity (%)	Bulk Density (Mg/m³)	Water Content (%)	Porosity (%)	Bulk Density (Mg/m³)	Shear Strength (kPa)	Parallel	Normal
Hole 490 (Cont.)																	
29	3	93–97	269.45						28.3[a]	52.5	1.86						
29	4	91–94	270.92						26.8	49.15							
30	1	50–53	275.0						21.9	42.54							
30	2	50–53	277.0						25.3	47.21							
30	3	10–14	278.10						27.1[a]	49.3	1.82						
31	2	23–27	284.75						26.2[a]	48.3	1.84						
33	1	93–97	299.95						22.7	43.67							
35	1	115–118	314.15						20.0	39.76							
35	2	87–91	315.40														
35	3	98–102	317.00														
35	4	123–127	318.75						20.7	40.80							
35	5	43–46	319.95									29.0	43.61	1.96			
36	1	138–141	323.90						22.4[a]	43.2	1.93						
36	3	132–135	326.85						22.9	43.95							
36	5	130–135	329.85						20.1	39.91							
37	1	87–91	332.90						21.8[a]	42.6	1.96						
37	2	94–97	334.45						23.3	44.51							
38	2	77–80	342.30						23.4[a]	44.9	1.92						
38	4	88–92	346.90						23.7[a]	45.3	1.91						
38	5	87–91	348.40						22.0	42.68							
39	1	81–83	351.82						21.2	41.53							
39	4	50–53	356.00						24.3	45.87							
39	6	81–84	359.30						21.12[a]	42.00	1.95						
40	4	60–63	365.00														
40	5	87–91	367.4						20.4	45.47							
40	7	32–35	369.85						22.0[a]	42.7	1.94						
41	1	138–141	371.40									28.1	39.34	2.01			
41	2	45–47	371.95						20.9	41.09							
42	1	50–53	380.00						20.7[a]	41.3	1.99						
42	4	88–92	384.90						19.4	38.85							
43	1	74–76	389.75						20.1[a]	40.3	2.01						
43	1	101–103	390.02						16.96[a]	35.6	2.10						1.884
43	2	78–82	391.30						20.3[a]	40.8	2.01						
43	3	68–71	392.70						20.9[a]	41.3	1.98						
43	3	118–121	393.20						23.0								
44	1	120–123										30.3	43.40	1.96			
44	1	123–125	399.75						21.8[a]	42.6	1.96						
44	2	108–112	401.10						19.9								1.816
44	2	47–49	400.48						22.8[a]	43.8	1.92						
47	1	62–65	418.18									23.80	37.07	2.05			
47	1	65–68	418.18						17.9[a]	36.4	2.04					1.812	
47	1	108–112	418.60						18.5[a]	37.3	2.02						
48	1	142–145	428.45						16.7[a]	34.61	2.09						1.708
48	1	142–145	428.45														
49	1	123–127	437.75						15.6[a]	32.0	2.11						
49	2	91–93	438.92						16.3	33.96							
49	2	91–93	438.92														
50	1	62–64	446.64						15.5[a]	32.8	2.11						
50	CC	5–7	455.05			1.97		43.64									
51	1	81–83	456.3			1.97		43.64	22.5[a]	43.4	1.93						
52	CC	5–7	465.55						17.2[a]	35.6	2.07						
53	1	73–76	475.25						19.9[a]	39.4	1.98						
53	1	88–91	475.40														
54	1	105–108	485.05			2.08		37.19	16.5	34.28							
54	2	41–43	485.92						17.6	36.06						1.884	
54	3	65–67	487.65						19.6[a]	39.3	2.00						
54	4	54–57	489.05						17.7[a]	36.5	2.06						
55	1	123–127	494.75						17.3	35.58							
55	2	138–141	496.40						20.1[a]	40.0	1.99						
55	3	107–110	497.60						16.1	34.61							
55	4	27–31	498.30			2.07		37.86	19.2	38.55						1.844	
55	4	65–67	498.65									21.5	35.83	2.072			
56	2	116–119	505.70									21.6	36.52	2.070		1.807	
56	3	93–96	506.95						19.0[a]	38.5	2.03						
56	4	92–96	508.45			2.14		33.45	18.8	37.94							
56	5	110–112	510.10						18.7[a]	38.0	2.03						
57	1	14–17	512.65						18.5	37.47							
57	1	108–111	513.6														
57	2	66–69	514.68			2.07		37.75	18.8[a]	38.1	2.03						1.796
57	3	49–52	516.00														
57	4	112–115	518.15						16.4[a]	34.4	2.10						
57	5	75–78	519.25														
57	6	108–111	520.10						21.5	41.96							
58	3	73–76	525.75														
58	3	143–147	526.45						22.0	42.68							
58	4	93–96	527.45						19.7[a]	39.8	2.02						1.726
58	5	86–89	528.88														
58	5	147–150	529.50			2.11		35.00									
58	6	65–68	530.15						16.9[a]	35.4	2.09						
59	2	96–99	533.98			2.12		34.5	20.5	40.50							
59	3	50–53	535.0						21.1[a]	40.4	2.01						
59	4	60–62	536.60						18.5	37.47							1.798
60	1	82–84	541.83						16.5[a]	34.7	2.11						
60	2	58–62	543.10														
60	2	72–74	543.23			2.03		40.11	20.9	41.09							1.708
60	4	38–41	545.90														
61	1	131–133	551.82						18.9	38.09							
61	2	75–77	552.75						18.6[a]	38.0	2.05						
61	3	50–53	554.0			2.10		35.9	19.1	38.40							1.799
61	4	56–58	555.57														
62	1	40–42	560.40						22.2	42.97							

				Continuous GRAPE		Two-Minute GRAPE			Rock Chunk or Gravimetric[a]			Air Pycnometer				Velocity (km/s)	
Core	Section	Interval (cm)	Sub-bottom Depth (m)	Bulk Density (Mg/m^3)	Porosity (%)	Bulk Density (Mg/m^3) Parallel	Bulk Density (Mg/m^3) Normal	Porosity (%)	Water Content (%)	Porosity (%)	Bulk Density (Mg/m^3)	Water Content (%)	Porosity (%)	Bulk Density (Mg/m^3)	Shear Strength (kPa)	Parallel	Normal
Hole 490 (Cont.)																	
62	3	50–53	563.5						21.4	41.82							
62	4	121–123	565.72														
62	4	50–53	565.0						21.2[a]	41.8	1.97						1.792
63	1	107–109	570.58						23.1	44.23							
63	2	63–65	571.65						22.0[a]	42.8	1.95						
63	2	128–130	572.30														
64	2	18–20	580.7						25.9[a]	47.8	1.84						
Hole 491																	
1	1	49–51	0.50				1.58	66.6	44.3	67.84					13.65		
1	2	113–116	2.65						41.6	65.39					23.39		
1	3	125–128	4.25									42.53	65.63	1.59	28.93		
1	4	127–130	5.80						40.3	64.16					33.24		
1	5	57–60	6.60						41.3[a]	65.3	1.58				31.70	1.529	
1	5	90–93	6.90				1.67	61.28	40.1	63.97							
2	2	135–137	11.35						41.7	65.48					44.73		
2	3	110–113	14.10						37.87[a]	62.2	1.64				24.21		
2	4	27–30	14.80						38.8	62.70					49.86		
2	4	85–87	15.35				1.77	55.81	36.9	60.79							
2	4	119–122	15.70						35.6	59.44					46.78		
2	4	145–147	15.95									37.46	61.40	1.651	34.19		
2	5	7–10	16.10						35.6[a]	59.9	1.66				35.90	1.529	
3	1	130–133	20.80						30.9	54.24					41.45		
3	2	102–105	22.05				1.73	57.74	32.6	56.18					51.91		
3	3	113–116	23.65						35.2	59.02					40.63		
3	4	18–21	24.20						36.3[a]	60.1	1.66				43.71		
3	6	31–34	27.33									33.64	56.73	1.722	56.22		
3	7	33–36	28.85				1.78	54.66	33.7[a]	56.9	1.70				56.73		
4	4	96–98	34.47				1.79	54.63	33.6	57.29					32.42		
4	5	45–48	35.45						33.2	56.85					60.57		
4	5	123–126	36.25				1.75	56.99	35.5	59.33					65.66		
4	CC	13–15	38.15						36.2[a]	59.7	1.65						
5	3	110–113	42.10						28.4	51.25					84.54		
5	3	118–120	42.20									29.13	52.06	1.820			
5	4	47–50	43.00						31.0[a]	54.3	1.75				105.06		
6	2	76–79	49.76				1.85	50.67	29.3	52.35					107.49		
6	3	48–50	51.00									35.23	58.55	1.69			
6	3	97–100	51.50						32.7[a]	56.1	1.72				90.56		
6	4	82–85	52.85						31.5	54.93					68.47		
6	5	99–102	54.5						30.9	54.24					78.16		
6	6	83–85	55.85				1.89	48.15	26.7	49.12							
6	7	8–11	56.60						35.0[a]	58.5	1.67						
7	1	99–102	58.5						26.9	49.38					109.91		
7	2	119–122	60.20												85.49		
7	3	111–114	61.13						33.6[a]	56.8	1.69						
7	4	48–51	62.50						29.3	52.35					87.93		
7	5	71–74	64.23						28.5	51.37					107.47		
7	6	89–92	65.90						29.7[a]	52.6	1.76				87.93		
7	7	9–12	66.60				1.83	52.12	27.5	50.13					122.12		
8	1	109–112	68.10						22.6	43.64					124.57		
8	2	132–135	69.85						30.2	53.43							
8	4	106–109	72.56						24.5	46.25							
8	5	136–139	74.36									25.09	46.62	1.90			
8	6	128–131	75.80						26.4[a]	48.7	1.84						
9	1	139–142	77.90						21.7	42.36							
9	2	113–116	79.15						27.5	50.15							
9	3	99–102	80.50						27.0[a]	49.3	1.82						
9	5	48–51	83.00						24.5	46.25							
9	7	10–13	85.60						28.0[a]	50.5	1.80						
10	5	79–82	92.80						24.5	46.25							
10	6	69–72	94.20						23.9	45.44							
11	2	117–120	98.20						24.5	46.25							
11	3	77–80	100.80						27.8[a]	50.5	1.81						
14	3	59–62	118.10						26.3	48.62							
14	6	55–58	122.55						21.6	42.22							
15	1	98–101	125.0						25.7[a]	47.3	1.84						
15	4	99–102	129.5				1.94	45.44	22.1	42.93							
15	5	98–101	131.0						21.7	42.36							
15	7	21–23	133.21						26.3[a]	48.3	1.84						
16	1	119–122	134.70						26.7	49.14							
16	4	72–75	138.75						25.1[a]	46.6	1.86						
16	4	108–111	139.10						21.7	42.36							
16	5	88–91	140.4						22.6	43.64							
16	6	68–71	141.70						16.7	34.71							
16	6	98–100	142.00									22.40	37.02	2.04			
16	6	108–111	142.10						19.72[a]	38.9	1.97						
17	1	101–103	144.01						22.5	43.50							
17	2	112–114	145.6						24.0	45.58							
17	4	115–118	148.65						27.04[a]	48.6	1.80						
17	5	100–102	150.00									29.70	43.69	1.93			
17	5	125–127	150.25						20.9	41.20							
17	6	38–41	150.90				2.015	40.90	22.3	43.22							
17	6	138–141	151.90						25.3[a]	46.5	1.84						
18	CC	12–14	161.62						21.5	42.07							
19	1	147–150	163.35						24.9	46.79							
19	3	35–38	165.35						21.9	42.65							
19	5	138–141	167.40						21.2[a]	41.8	1.97						
21	3	101–104	185.01						18.6	37.73							
21	3	134–137	185.35						20.9[a]	41.1	1.97						
21	4	7–10	185.60									26.69	40.53	1.99			
22	4	03–07	195.05						25.9[a]	49.5	1.91						
22	4	145–147	196.45						18.9	38.20							

Core	Section	Interval (cm)	Sub-bottom Depth (m)	Continuous GRAPE Bulk Density (Mg/m^3)	Continuous GRAPE Porosity (%)	Two-Minute GRAPE Bulk Density (Mg/m^3) Parallel	Two-Minute GRAPE Bulk Density (Mg/m^3) Normal	Two-Minute GRAPE Porosity (%)	Rock Chunk or Gravimetric[a] Water Content (%)	Rock Chunk or Gravimetric[a] Porosity (%)	Rock Chunk or Gravimetric[a] Bulk Density (Mg/m^3)	Air Pycnometer Water Content (%)	Air Pycnometer Porosity (%)	Air Pycnometer Bulk Density (Mg/m^3)	Shear Strength (kPa)	Velocity (km/s) Parallel	Velocity (km/s) Normal
Hole 491 (Cont.)																	
23	2	39–41	200.90						18.8	38.04							
25	1	143–146	210.95						21.2	41.64							
25	2	31–34	211.33						22.8[a]	43.5	1.91						
25	3	48–51	213.0						22.8	43.92							
25	5	31–34	215.31						23.1[a]	44.0	1.91						
25	5	135–137	216.35									31.10	45.45	1.93			
25	6	81–84	217.82				2.01	41.30	22.5	43.50							
26	2	109–112	221.60				2.05	39.1	23.1[a]	43.9	1.91						
26	3	127–131	223.30						20.5	40.61							
26	5	108–111	226.10						20.3	40.48							
26	6	137–140	227.90						22.4[a]	46.0	1.92						
27	3	123–127	232.75						24.5[a]	45.8	1.87						
27	4	118–121	234.20				2.00	41.67	21.3	41.79							
27	5	141–145	235.95						20.4	40.46							
27	7	16–19	237.65						20.99[a]	40.9	1.95						
28	2	106–109	240.56														
28	4	125–135	243.75						24.1	45.71							
28	5	49–59	244.55						24.7[a]	46.6	1.88						
28	5	66–69	244.70				2.04	39.26	17.6	36.16							
29	3	99–102	251.50						19.7	39.42							
29	4	91–94	251.91						20.9[a]	41.0	1.96						
29	5	96–99	254.45				2.12	34.62	17.7	36.32							
30	2	58–60	259.10						18.6	37.73							
30	3	95–97	260.95				1.94	45.35	18.9	38.20							
30	4	43–45	261.95									28.00	41.98	1.97			
30	4	81–83	262.36						24.8[a]	46.4	1.87						
30	6	121–123	265.22						18.95[a]	38.0	2.00						
31	6	32–35	274.35						20.6[a]	40.2	1.95						
33	1	134–137	286.35						24.1[a]	45.2	1.88						
33	2	1–4	286.52						21.66[a]	42.1	1.94						
33	6	103–106	294.05						22.3[a]	42.9	1.93						
34	6	16–20	302.70						22.1[a]	42.6	1.93						
35	5	52–54	311.02						20.5[a]	40.7	1.98						
36	4	83–86	319.35						22.14[a]	42.6	1.92						
36	5	147–150	321.50						23.5[a]	44.5	1.89						
37	4	143–147	329.45						20.6[a]	40.4	1.96						
37	4	145–148	329.48						20.1	40.02							
38	1	89–92	330.90														
38	2	37–41	331.90						26.2[a]	47.9	1.83						
38	2	55–58	332.05														
38	2	84–87	332.35														
38	2	105–108	332.55				1.876	49.18									
39	1	89–91	340.40						21.4[a]	41.8	1.96						
40	2	106–109	354.56						21.9[a]	42.1	1.92						
40	3	30–33	355.30				2.030	40.0	19.3	38.81							
39	2	84–87	341.85						21.02[a]	41.14	1.96						
41	5	52–54	368.02						19.4	38.96							
41	5	94–97	368.45				2.049	38.86	19.4	38.96							
41	3	55–58	365.05						22.6[a]	43.2	1.91						
43	2	147–150	384.5						19.9[a]	39.4	1.98						
43	4	58–61	386.10						15.4	32.56							
44	3	109–112	394.10						17.7	36.32							
44	4	22–24	394.72						21.4[a]	41.9	1.96						
45	3	52–55	403.07						20.8	41.06							
45	4	13–16	404.20						22.4[a]	43.0	1.92						
46	1	138–141	410.4						21.1	41.49							
48	2	143–147	430.95						19.3[a]	38.5	2.00						
48	4	88–92	433.40						16.7	34.71							
49	3	51–53	441.01						18.6[a]	37.6	2.02						
50	3	48–51	451.50						19.0[a]	38.2	2.01						
50	4	60–63	453.10						18.9	38.20							
50	5	13–16	454.15						17.8[a]	36.1	2.03						
51	2	69–71	459.70						18.0	36.80							
51	3	5–7	460.55						16.9	35.04							
51	4	16–19	462.16						17.7[a]	36.2	2.05						
52	3	17–19	469.18						17.1[a]	35.6	2.08						
53	1	50–53	478.00														
53	CC		483.90						17.3[a]	35.6	2.06						
54	1	92–95	485.95						17.1	35.36							
54	3	31–33	488.31						17.9[a]	36.6	2.04						
55	1	131–133	495.32						17.1	35.36							
55	2	79–82	496.30						17.2[a]	35.4	2.06						
55	3	58–61	497.60														
56	1	79–81	504.8														
56	2	46–49	504.47						19.4	38.96							
56	3	69–71	507.70						17.9[a]	36.4	2.03						
57	3	48–51	517.00						15.7	33.06							
57	4	33–36	518.35						16.9[a]	35.0	2.07						
57	5	14–17	519.65									22.02	35.78	2.08			
58	2	13–16	524.65						15.11[a]	32.2	2.13						
58	3	108–111	527.10						16.9	35.04							
59	1	56–57	533.06						18.4[a]	37.1	2.02						
59	CC	0–02	533.50									20.8	34.69	2.08			
Hole 492																	
1	1	48–51	0.50						52.4	74.57							
1	1	138–141	1.40						48.6	71.57					58.9		
1	2	9–12	1.60	1.79	54.32				46.4	69.75							
1	2	48–50										100.0	72.04	1.46			
1	2	117–120	2.70						43.4	67.13							
1	3	9–12	3.10						43.5	67.22					11.41		

				Continuous GRAPE		Two-Minute GRAPE			Rock Chunk or Gravimetric[a]			Air Pycnometer				Velocity (km/s)	
Core	Section	Interval (cm)	Sub-bottom Depth (m)	Bulk Density (Mg/m³)	Porosity (%)	Bulk Density (Mg/m³) Parallel	Bulk Density (Mg/m³) Normal	Porosity (%)	Water Content (%)	Porosity (%)	Bulk Density (Mg/m³)	Water Content (%)	Porosity (%)	Bulk Density (Mg/m³)	Shear Strength (kPa)	Parallel	Normal
Hole 492 (Cont.)																	
2	2	130-133	6.30	1.58	66.7				43.5	67.22					14.73		
2	3	74-76	7.25									68.80	65.57	1.60	25.40		
2	3	119-122	7.20						38.7	62.70					28.35		
2	4	13-16	8.15	1.66	61.70				42.0	65.8	1.57						
2	4	81-84	8.80						37.3	61.30					41.97		
3	2	110-113	16.60	1.78	54.71				36.7	60.69					58.90		
3	3	117-120	17.20						26.4	50.5	1.91				93.99		
3	4	17-20	17.70	1.76	55.98				26.8	51.86					46.9		
3	4	96-99	18.45						33.3	57.07					70.68		
3	4	148-150	19.19									45.82	55.76	1.79			
3	5	16-19	19.19						35.7	59.65							
3	5	52-55	19.55						34.3[a]	58.4	1.70				94.24		
4	1	105-108	23.55						35.3	59.13					47.49		
4	6	23-26	30.25	1.72	58.5				35.9	59.86					63.5		
4	6	125-128	31.25						34.9	58.81					153.14		
4	7	34-37	31.85						34.8[a]	58.7	1.69				121.48		
4	CC	10-12	31.95						34.1	57.95					54.71		
5	1	137-140	33.40						38.0	62.01					62.58		
5	2	18-21	33.70	1.67	61.7				37.3	61.30					55.69		
5	2	137-140	34.90						39.2[a]	62.5	1.60				69.94		
5	3	50-52	35.70									58.81	62.23	1.64			
5	3	121-124	36.22	1.65	62.9				34.6	58.49					72.15		
5	4	95-98	37.45						36.3[a]	59.5	1.64						
5	4	108-111	37.58														
5	5	99-101	39.00												116.33		
5	4	18-21	35.70						33.2	56.96							
5	5	9-11	38.10						24.6	46.49							
6	1	135-138	42.85						25.0	47.03					106.76		
6	2	22-25	43.25						35.3[a]	58.9	1.67						
6	2	108-110	44.10									50.00	55.93	1.70			
6	4	136-139	47.36						31.6	55.16					112.36		
6	5	48-50	48.00									36.80	49.18	1.89			
6	5	120-123	48.7	1.77	55.3				29.8	53.06					109.91		
6	6	71-74	49.74						29.02[a]	52.0	1.79				119.68		
7	3	33-36	54.35						31.5[a]	54.5	1.74						
7	3	53-56	54.55						27.2	49.87							
8	1	99-102	61.5						22.5	54.60							
8	2	29-32	63.30						25.7	47.95							
8	3	57-60	64.10	1.84	51.53				28.3[a]	50.9	1.80						
8	3	110-112	64.60									39.90	50.37	1.88			
8	4	57-60	65.60						26.9	49.19							
9	2	93-96	72.45	1.76	55.9				32.8[a]	55.9	1.71						
9	3	24-27	73.25						27.6	50.38							
10	1	36-39	79.89						23.1	44.44							
10	3	53-57	83.05						24.6	46.49							
10	4	100-103	84.0						26.6[a]	48.9	1.84						
11	1	29-31	89.3						21.8	42.61							
11	2	85-88	91.35	1.86	50.3				27.0[a]	49.9	1.84						
11	2	148-150	92.00									33.60	47.43	1.92			
11	3	57-60	92.60						22.9	44.16							
11	CC	1-4	98.02						26.8[a]	49.5	1.84						
12	1	128-131	99.80						24.0	45.68							
12	2	98-101	101.0	1.86	50.1							33.60	45.30	1.89			
12	3	62-64	102.14						27.4[a]	49.7	1.81						
12	4	48-50	102.40									35.03	47.50	1.90			
12	4	106-109	103.06						25.0	47.03							
12	5	42-44	104.94	1.87	49.6				25.1	47.16							
13	2	110-113	110.6						26.1[a]	48.6	1.86						
13	3	12-15	111.15						26.0	48.34							
14	1	135-137	118.85														
14	3	67-70	121.2						25.8	48.08							
14	3	113-116	121.65									38.60	50.54	1.85			
14	3	142-145	121.95						26.0	48.34							
14	5	121-125	124.75						26.7	49.24							
14	6	136-139	126.39						27.7[a]	50.4	1.82						
15	1	67-70	127.7						31.2[a]	54.4	1.75						
15	2	95-98	129.45						25.0	47.03							
15	3	113-116	131.15						27.8	50.63							
16	3	28-31	139.80						28.8[a]	52.1	1.81						
16	4	0-3	141.03						32.3	55.96							
16	5	19-22	142.70						27.3	50.00							
16	5	22-25	142.75						28.1[a]	51.0	1.81						
16	CC	2-5	145.55									41.30	51.38	1.82			
17	1	13-16	146.15						31.4[a]	54.7	1.74						
17	1	118-121	147.20						30.5	53.89							
17	3	13-15	149.15									42.59	52.67	1.80			
17	3	15-17	149.15						30.4	53.77							
18	1	91-94	156.44						30.1	53.42							
18	3	56-59	159.06						31.1[a]	54.1	1.74						
18	3	98-101	159.50						29.4	52.58							
18	4	51-54	160.51						31.3	54.82							
18	CC	0-3	164.53									37.40	48.75	1.87			
19	1	147-150	166.5						30.8	54.24							
19	2	13-16	166.65						31.1[a]	54.4	1.75						
19	3	84-87	168.85						30.6	54.01							
22	3	73-75	197.25									37.70	49.74	1.84			
22	3	75-78	197.25						26.8[a]	49.1	1.83						
22	5	57-61	200.10						22.5	43.60							
23	1	23-25	203.25									33.60	47.59	1.89			
23	4	138-141	208.5						23.4	44.86							
23	CC	0-2	212.03						25.7[a]	47.6	1.85						

				Continuous GRAPE		Two-Minute GRAPE			Rock Chunk or Gravimetric[a]			Air Pycnometer				Velocity (km/s)	
						Bulk Density (Mg/m³)											
Core	Section	Interval (cm)	Sub-bottom Depth (m)	Bulk Density (Mg/m³)	Porosity (%)	Parallel	Normal	Porosity (%)	Water Content (%)	Porosity (%)	Bulk Density (Mg/m³)	Water Content (%)	Porosity (%)	Bulk Density (Mg/m³)	Shear Strength (kPa)	Parallel	Normal
Hole 492 (Cont.)																	
24	1	111-113	212.61						20.0[a]	39.9	2.00						
24	2	4-6	214.05						21.7[a]	42.3	1.95						
24	3	34-36	215.85									30.21	43.31	1.96			
24	3	58-62	216.10						25.11	47.17							
24	CC	1-3	221.53						22.9	44.16							
25	1	24-27	222.25						22.6[a]	43.8	1.94						
25	3	101-104	226.01						19.3	38.91							
25	4	45-48	226.95									26.20	39.92	2.03			
25	5	81-84	228.81						18.3	37.36							
26	2	91-93	233.91						22.3	43.32							
26	4	56-59	235.59						23.9[a]	45.6	1.91						
26	5	98-100	237.50									25.09	39.00	2.06			
26	6	17-20	239.20						22.1[a]	42.6	1.93						
27	1	5-7	241.05						24.5[a]	46.1	1.88						
27	1	130-132	242.30									32.61	45.12	1.93			
27	2	72-75	243.25						23.9[a]	45.5	1.90						
27	4	69-72	246.20						25.8	48.08							
29	4	56-59	265.06						15.6[a]	32.8	2.10						
29	4	66-69	265.16									16.40	28.96	2.19			
29	4	83-86	265.35						15.2	32.31							
30	1	50-52	265.50									27.60	42.82	1.98			
30	2	19-21	266.70									22.59	36.75	2.07			
31	1	118-121	270.7						21.5[a]	42.2	1.96						
Hole 492A																	
1	1	29-32	0.30						50.1	72.78					8.62		
1	1	79-82	0.80						47.2[a]	69.4	1.47				15.39		
1	1	109-112	1.10									89.8	69.49	1.51	18.06		
1	1	140-143	1.40						44.8	68.37					23.19		
1	2	20-23	1.70	1.60	65.5				44.5	68.10					24.83		
1	2	56-58	2.06						43.5[a]	66.2	1.52						
1	2	60-63	2.10												28.10		
1	2	80-83	2.30									80.2	67.21	1.55	26.67		
1	2	120-123	2.70						45.4	68.89					22.47		
1	3	19-22	3.20						46.1	69.49					11.49		
1	3	39-42	3.40												8.62		
1	3	59-62	3.60						43.4	67.13					7.18		
1	3	79-82	3.80						42.6	66.40					8.93		
2	1	89-92	5.15	1.69	60.4				41.8	65.67	1.57				18.77		
2	1	119-122	5.45						40.8	63.97					53.01		
2	1	139-140	5.65									69.2	63.28	1.60	18.77		
2	2	19-22	5.95	1.63	63.6				41.2	65.11					47.86		
2	2	59-62	6.35									67.8	63.82	1.61	50.07		
2	2	89-92	6.65						39.4[a]	62.5	1.59				52.27		
2	2	119-122	6.95						41.9	65.76					53.75		
2	3	24-26	7.50						39.2	63.19					67.00		
2	3	49-52	7.75						39.6	63.58					68.47		
2	3	73-76	8.00						40.7[a]	64.2	1.58				57.43		
3	1	20-25	9.20									62.1	62.07	1.64			
3	1	59-62	9.60						36.9	60.90					36.07		
3	1	89-92	9.90						35.0[a]	59.0	1.68				71.78		
3	1	119-122	10.20						37.9	61.91					58.16		
3	1	148-150	10.50									62.1	61.73	1.64			
3	2	09-12	10.60						36.6	60.59							
3	2	35-38	10.85									54.6	58.70	1.69	76.57		
3	2	41-42	10.91						35.9[a]	59.4	1.65				73.63		
4	1	69-72	14.45						34.0	57.84					30.19		
4	1	89-92	14.65						33.3[a]	57.4	1.72				48.59		
4	1	119-122	14.95						33.1	56.85					71.05		
4	2	02-05	15.30									49.7	56.40	1.74			
4	2	21-23	15.45						36.2						57.43		
4	2	61-63	15.86						37.5[a]	61.0	1.63				80.99		
5	1	44-47	23.70						34.5	58.38					86.14		
5	1	69-72	23.95												96.45		
5	1	109-112	24.35						34.3[a]	57.7	1.68				100.13		
5	1	139-142	24.55						35.1	59.02					62.58		
5	2	14-17	24.90						33.1[a]	56.5	1.71				108.23		
5	2	59-62	25.35						34.7	58.59					128.8		
5	2	108-110	25.85									52.3	58.72	1.72			
5	2	100-112	25.85						28.0	50.88					152.4		
5	2	139-142	26.15						34.7[a]	58.5	1.68				122.22		
6	1	75-78	28.75									52.9	58.23	1.72	137.68		
6	1	129-132	29.30						34.9[a]	56.90	1.68				147.7		
6	2	29-32	29.80						35.7[a]	59.5	1.67				180.4		
6	2	88-90	30.40									53.6	57.81	1.72			
6	2	118-121	30.70						33.6	57.40							
7	1	34-37	33.10						36.1[a]	59.8	1.66						
7	1	79-82	33.45									51.7	57.86	1.71			
7	1	123-127	33.90						30.5	53.89					179.65		
7	2	8-11	34.35	18.3	52.2				35.9[a]	59.6	1.66				156.09		
7	2	58-61	34.85						33.0						192.16		
8	1	59-62	38.10						33.9[a]	57.9	1.71						
8	1	106-108	38.56						35.9[a]	59.5	1.66						
9	1	61-63	42.86						28.2[a]	51.1	1.81						
9	1	83-85	43.10						25.0	47.03							
10	1	3-5	47.05									44.3	52.98	1.79			
10	1	5-7	47.05						30.1	53.42							
10	1	32-34	47.34						35.2[a]	58.4	1.66						
10	1	143-146	48.45						28.0	50.88							
11	1	66.05							30.3[a]	53.7	1.77						

				Continuous GRAPE		Two-Minute GRAPE			Rock Chunk or Gravimetric[a]			Air Pycnometer				Velocity (km/s)	
						Bulk Density (Mg/m³)											
Core	Section	Interval (cm)	Sub-bottom Depth (m)	Bulk Density (Mg/m³)	Porosity (%)	Parallel	Normal	Porosity (%)	Water Content (%)	Porosity (%)	Bulk Density (Mg/m³)	Water Content (%)	Porosity (%)	Bulk Density (Mg/m³)	Shear Strength (kPa)	Parallel	Normal
Hole 493																	
2	1	49-52	120.50						31.2	54.22					136.8		
2	2	64-67	122.15						31.6	54.68					109.9		
2	3	71-73	123.71						33.7[a]	56.0	1.66						
2	3	148-150	124.50									31.13	53.52	1.74			
3	1	78-81	130.3						28.6	51.13							
3	1	109-112	130.60						34.2[a]	56.7	1.66						
3	2	88-90	131.90						30.8	53.76							
4	2	30-32	140.80						30.3	53.17							
5	1	81-83	149.31						33.5	56.82							
5	2	70-73	150.70						32.6[a]	55.0	1.69						
5	3	82-84	152.32						29.8	52.58							
5	4	91-94	153.91						30.6	53.53							
6	2	130-133	160.8						32.1	55.25							
7	2	100-103	170.0						31.4	54.45							
8	3	56-58	180.56						32.8	56.04							
9	1	100-104	187.5						28.7	51.25							
9	3	40-43	189.9						33.7[a]	55.6	1.65						
9	5	20-23	192.7						28.5	51.01							
10	1	23-26	196.25						29.1	51.74							
10	2	51-53	198.01						33.8[a]	56.2	1.66						
10	3	40-43	199.40						30.9	53.88							
10	5	12-17	202.15						31.2	54.22							
11	1	124-127	206.75	1.85	50.9				34.0[a]	56.4	1.66						
11	2	67-70	207.70						31.8	54.91							
13	1	66-69	225.19						32.9[a]	54.5	1.66						
14	1	80-83	234.80						34.4[a]	56.8	1.65						
14	2	37-41	235.90						29.6	52.34							
14	5	19-23	240.20						29.9	52.70							
15	1	100-102	244.5						31.6[a]	54.1	1.71						
15	3	99-101	247.5	1.84	51.5				28.9	51.50							
15	4	34-36	248.35						29.2	51.86							
17	1	126-129	263.79						31.3[a]	53.4	1.70						
17	2	31-35	264.35						23.4	44.38							
17	3	70-74	266.20						29.9	52.70							
17	3	135-138	266.80									25.32	46.56	1.86			
18	4	122-125	277.75	1.85	50.9				26.4	48.37							
18	5	85-88	278.85						26.8[a]	48.0	1.79						
18	6	91-94	280.43						31.9	55.03							
19	2	147-150	284.5						29.6	52.34							
19	4	147-150	287.5	1.87	49.6				26.8	48.88							
19	5	127-130	288.8						34.6[a]	57.1	1.65						
20	1	124-126	292.25						32.6	55.82							
20	3	100-103	295.0						32.3	55.48							
20	5	84-87	297.85						30.1	52.94							
20	7	36-38	300.36						24.4[a]	45.6	1.87						
21	2	102-104	303.04						24.9	46.41							
21	4	83-84	305.85	1.90	47.7				25.8	47.60							
21	5	65-67	307.15						31.1[a]	51.4	1.66						
22	1	43-45	311.15						28.6	51.13							
22	3	104-106	314.05						28.6	51.13							
22	4	46-48	314.96						28.1[a]	49.5	1.76						
22	5	71-73	316.71						30.8	53.76							
23	CC	03-05	328.55						26.6	48.63							
24	1	112-114	330.12						26.2	48.11							
24	2	109-112	331.14						28.4[a]	49.5	1.74						
24	3	78-81	332.80	1.80	53.4				24.5	45.88							
25	1	123-125	339.75						31.1	54.11							
25	3	133-136	342.85	1.85	51.7				28.4	50.89							
25	4	102-104	344.03						27.7[a]	49.2	1.78						
25	5	125-127	345.75						29.5	52.22							
26	2	94-97	350.45						27.5	49.77							
27	1	124-126	358.75						30.3	53.17							
27	2	96-98	359.97						26.7[a]	47.9	1.79						
27	4	83-85	362.85						22.5	43.13							
27	4	131-133	363.32						22.5[a]	43.13	1.95						
27	5	128-130	364.80						21.7	41.99							
28	1	142-145	368.45						21.7	41.99							
28	3	109-112	371.10						16.9	34.69							
28	4	84-87	372.35						21.98[a]	42.9	1.95						
28	5	148-150	374.50						19.7	39.05							
29	1	94-98	377.45						20.8	40.69							
29	2	35-37	378.35	1.86	50.3				20.6	40.39							
29	3	46-50	380.0						25.2[a]	47.4	1.88						
29	5	27-31	382.80						21.9	42.28							
30	1	66-69	386.66						21.2	41.27							
30	3	40-44	389.40						22.9[a]	44.3	1.93						
30	4	47-50	391.0						19.8	39.20							
30	5	96-100	393.0						22.4	42.99							
30	6	54-58	394.05						22.6	43.27							
31	1	78-82	396.30						31.1	54.11							
31	2	27-31	397.30						34.2[a]	45.8	1.90						
31	3	33-36	398.85						22.7	43.41							
31	5	62-66	402.15						22.7	43.41							
31	6	42-46	403.45						24.3	45.61							
32	1	92-95	405.95						21.7	41.99							
32	2	4-7	406.55						21.3[a]	41.9	1.96						
32	3	123-127	409.25	1.95	44.5				26.4	48.37							
33	1	74-77	415.25						29.4[a]	51.8	1.76						
33	2	7-10	416.10						23.7	44.79							
33	3	113-116	418.65						20.9	40.83							
33	6	106-109	420.05						19.5	38.75							

				Continuous GRAPE		Two-Minute GRAPE			Rock Chunk or Gravimetric[a]			Air Pycnometer				Velocity (km/s)	
Core	Section	Interval (cm)	Sub-bottom Depth (m)	Bulk Density (Mg/m^3)	Porosity (%)	Bulk Density (Mg/m^3) Parallel	Normal	Porosity (%)	Water Content (%)	Porosity (%)	Bulk Density (Mg/m^3)	Water Content (%)	Porosity (%)	Bulk Density (Mg/m^3)	Shear Strength (kPa)	Parallel	Normal
Hole 493 (Cont.)																	
34	2	102–104	426.04						19.7[a]	39.5	2.01						
34	3	106–109	428.06						19.3	38.45							
34	4	50–53	429.0						19.8	39.20							
34	5	14–16	430.15	2.00	42.0				19.6	38.9							
34	6	30–32	431.80						15.9	33.06							
35	1	143–146	434.95						20.8[a]	41.5	2.00						
35	2	145–147	446.45						16.8	34.53							
35	6	12–14	441.12						16.5	34.04							
36	1	148–150	444.50						18.4	37.07							
36	3	138–140	447.40						19.1	38.15							
36	4	119–121	448.70						19.1[a]	38.5	2.02						
37	1	98–100	453.5						18.7	37.53							
37	2	94–96	454.95						18.6[a]	38.4	2.06						
37	4	105–107	458.05						18.7	37.53							
38	1	62–64	462.62						15.4	32.23							
38	3	100–104	466.0						16.2	33.55							
38	2	78–81	464.30						16.0[a]	33.5	2.10						
39	1	106–108	472.58						18.6	37.38							
39	2	133–136	474.35						20.3[a]	40.2	1.98						
39	3	104–106	475.55						20.6	40.39							
40	1	123–125	482.25						17.5	35.65							
40	2	28–31	482.80						16.5	34.04							
41	1	76–78	491.25						15.3	32.06							
41	2	64–66	492.65						18.2	36.76							
41	2	118–120	493.20						17.7[a]	36.5	2.07						
42	1	141–143	501.43						20.3	39.95							
42	2	136–138	502.85						20.4[a]	41.1	2.02						
42	4	90–93	505.40						20.9	40.83							
42	3	142–144	507.42						19.3	38.45							
43	1	147–150	511.0						15.2	31.89							
43	3	147–150	514.0						16.3	33.72							
43	4	109–111	515.1						15.2[a]	32.5	2.14						
43	5	147–150	517.0						14.9	31.38							
44	1	145–147	520.45						16.9	34.69							
44	3	134–136	523.35						16.3	33.72							
44	5	88–91	525.90														
45	1	102–106	529.55						19.6	38.9							
45	2	95–97	530.95						19.6[a]	39.6	2.02						
45	3	126–129	532.76						13.2	28.43							
46	2	119–121	540.70						14.8	31.21							
46	3	119–121	542.20						15.3[a]	32.9	2.15						
46	4	105–108	543.55						15.3	32.06							
46	6	14–17	545.65						15.3	32.06							
47	1	28–31	547.80						22.0	42.42							
47	3	57–60	551.10						16.8[a]	35.5	2.11						
47	5	38–41	553.90						17.3	35.33							
48	1	15–18	557.15						17.2	35.25							
48	3	13–14	560.14						18.7	38.6	2.06						
49	1	9–12	566.60						17.2	35.25							
49	3	6–9	569.59						14.9	31.9	2.14						
49	7	5–8	575.55						16.1	33.39							
50	2	13–16	577.65						15.7[a]	32.3	2.05						
50	3	13–16	578.65						16.0	33.22							
Hole 493B																	
1	4	51–53	17.01	1.65	63.0				42.8						24.1		
2	1	115–118	22.65						43.8						27.8		
2	4	116–118	27.16						36.4	59.92							
3	4	135–138	36.85						33.5	56.82							
3	6	65–66	39.15						39.0[a]	62.5	1.60						
3	7	6–8	40.06						36.8	60.33							
4	4	144–146	46.45						31.0	53.99					37.55		
4	5	129–131	47.8						36.4	59.92					17.67		
5	1	111–118	51.15						39.5[a]	62.9	1.59				38.28		
5	2	27–29	51.78	1.69	59.8				35.6	59.08							
5	3	45–47	53.45						33.6	56.93					44.9		
6	2	113–115	62.15						36.6[a]	59.8	1.63				75.09		
6	3	116–118	63.68						34.2	57.58					104.54		
6	3	135–138	65.85									31.13	55.04	1.74			
6	4	45–47	64.45						30.13[a]	52.5	1.74				136.93		
7	1	144–146	70.45						35.7	59.19					72.15		
7	2	63–65	71.15						35.1[a]	58.5	1.67				68.47		
7	2	129–131	71.80						32.3	55.48					64.79		
8	1	93–95	79.45						34.3	57.69					70.68		
8	2	21–24	80.21						35.9[a]	58.5	1.65				46.38		
9	1	132–134	89.32						33.6	56.93					59.63		
10	1	83–86	98.35						33.5[a]	57.0	1.70				83.19		
10	CC	03–05	106.55						29.0	51.62							
11	1	147–150	118.0						32.9	56.15							
11	2	89–91	118.90						33.4[a]	56.7	1.70						
11	3	117–119	120.69						29.8	52.58					148.71		